PLASTIC RESPONSE IN *PINUS* SPP., DETERMINING THE TEMPORAL WINDOW OF RESPONSE AND SPECIES-LEVEL VARIATION OF UV-B ABSORBING COMPOUNDS TO SHORT-TERM VARIATION IN UV-B RADIATION

Advances in developing a pollen-based UV-B proxy using THM py-GC/MS

MARI JOKERUD

Thesis for the degree of philosophiae doctor (PhD)
University of Bergen

2017

Date of defence: 27.01.2017

Pinus nigra from The Lourizán Botanical Garden, Pontevedra, Spain.

Year: 2016

Title: Plastic response in *Pinus* spp., determining the temporal window of response and species-level variation of UV-B absorbing compounds to short-term variation in UV-B radiation.

Advances in developing a pollen-based UV-B proxy using THM py-GC/MS

Author: Mari Jokerud

Print: AIT Bjerch AS / University of Bergen

“The ever-changing display of plant forms, which I have followed for so many years, awakens increasingly within me the notion: The plant forms, which surround us, were not all created at some given point in time and then locked into the given form. They have been given a felicitous mobility and plasticity that allows them to grow and adapt themselves to many different conditions in many different places.

Johann Wolfgang von Goethe

Contents

Abstract

The total amount of ultraviolet radiation (UV-B wavelength = 280–315 nm) reaching the Earth' surface has probably experienced large changes throughout Earth's history. An untested hypothesis is that past variations in UV-B flux have had a significant impact on the tempo and mode of speciation and extinctions. To address the impacts of variability in exposure to surface UV-B radiation in the geological past, a proxy is required.

A pollen-based UV-B proxy, using a newly-developed thermally assisted hydrolysis and methylation pyrolysis-gas chromatography and mass spectrometry method (THM py-GC/MS), is proposed as a promising new proxy to reconstruct changes in past UV-B. However, measurements from py-GC/MS can have a high variance and, as a consequence, low analytical precision along with reproducibility issues over long analytical periods. Despite these challenges, previous work using pollen has established i) a general dose-response relationship between UV-B radiation and UV-B absorbing compounds, ii) a relationship between mean long-term UV-B and UV-B absorbing compounds across Europe and iii) a successful palaeoecological reconstruction of past UV-B flux across the Holocene using the THM py-GC/MS method.

Pollen development in *Pinus* spp. occurs one to two months before dehiscence. During this period the pollen grains are coated with UV-B absorbing compounds, and these compounds are produced to protect themselves from harmful UV-B radiation. In light of this, we investigated whether *Pinus* spp. pollen displays a plastic response to short-term changes in UV-B radiation by altering the production of UV-B absorbing compounds. We then further investigated whether this response could be pinpointed to a more accurate time period, e.g. weeks before dehiscence. Since *Pinus* species remain difficult to identify using traditional light microscopic methods, but have notably different pollen sizes, we wanted to investigate whether different *Pinus* species exhibit species-level variations in their production of UV-B absorbing compounds.

First, in order to improve analytical precision of the THM py-GC/MS method, we modified the method by adding an internal standard of Nonadecanoic acid to calculate

the *p*-Coumaric acid ratio (*p*CA). We developed a protocol adapted to analyse pollen from *Pinus* spp. by testing the effect of number of grains on *p*CA ratio and signal-to-noise ratio. In addition, we performed various tests on different sample preparations, machine settings and cleaning procedures. In order to answer whether *Pinus* spp. show a plastic response to UV-B, we conducted two experiments; (i) we artificially shaded one branch on ten trees with a 90% shading cloth one month before flowering. During dehiscence we collected pollen from the shaded and sun-exposed branches. (ii) We collected pollen from the same trees of several *Pinus* spp. in two consecutive years with natural variation in UV-B. These pollen samples were also used to investigate species-level variation between years. In order to investigate the timing of the response we collected *Pinus* pollen from 13 arboreta along a geographical gradient across Europe. We analysed our results using a Bayesian hierarchical model, which enabled us to take into account uncertainties in machine performance and pollen picking precision, which is a novel approach in this research area.

Our results include two major improvements of the THM py-GC/MS method; we introduced an internal standard which increased the analytical precision of the UV-B absorbing compounds by 50%, and by using calibration solutions we were able to detect and correct for drift in machine precision and between batches and column cuts. Number of pollen grains has a strong linear correlation with *p*CA ratio, and the highest signal-to-noise ratio was at 250 grains. We did not detect Ferulic acid which is another UV-B absorbing compound found in e.g. *Alnus* spp. pollen.

In the shading experiment the shaded pollen produced 21% less UV-B absorbing compounds than the sun-exposed pollen. In Geneva the UV-B radiation in April-May 2014 was 1034 J m^2 higher compared to April-May 2013, while there were minor differences in UV-B exposure between the two previous growing seasons. The pollen collected in 2014 consisting of multiple species contained 24% more UV-B absorbing compounds than pollen collected in 2013. The species from Geneva also displayed species-level variations. This was still apparent after applying corrections for a difference in biovolume. Lastly, the results from pollen collected across Europe show UV-B radiation during the last two weeks before dehiscence to be the best predictor

variable of UV-B absorbing compound production. The last two weeks prior to dehiscence had the lowest deviance information criterion (DIC) values and highest slope coefficients.

Our findings in both experiments demonstrate a plastic response of UV-B absorbing compounds to short-term changes in UV-B radiation. This is further supported in the broad scale study across Europe on timing of the response, which indicates that the amount of UV-B absorbing compounds is determined by the UV-B during the last two weeks before pollen dehiscence. During the last two weeks in pollen development, the tapetal cells produce the peritapetal membrane containing UV-B absorbing compounds which covers the pollen grain. Even though our pollen size corrections did not fully remove species-level variation, we expect measuring mean actual pollen size of a sample would remove these differences.

Our findings have implications for the usage of *Pinus* pollen and UV-B absorbing compounds as a proxy for past changes in UV-B flux; First our findings show that *Pinus* spp. exhibit a plastic short-term response to UV-B which suggests that the signal will reflect changes in local UV-B at the given site. Second, this short term response will provide a seasonal (spring-time) UV-B signal in palaeoecological reconstructions of changes in past UV-B. A typical sample from the pollen record represents anywhere between 5 and 20 years, and any between-year variation in pollen season UV-B is therefore averaged out, giving us confidence that we can observe long-term trends. Finally, the species-level variation observed in our study suggests that UV-B reconstructions may be more difficult in sediment cores sampled in an area with known occurrence of several species of *Pinus*. We expect that applying size corrections to *p*CA ratios could improve the accuracy of the reconstruction of past UV-B, especially if specific size-correction factors for a given site can be established. The results from this thesis are novel and contribute important implications for the THM py-GC/MC method and the use of a *Pinus* spp. pollen-based UV-B proxy. It opens the door for future investigations into the drivers of change of pollen-chemistry.

Acknowledgements

I want to thank Kathy Willis and Vigdis Vandvik for offering me the PhD position in the Parasol project. The novelty of the Parasol project and being in the frontier of developing a new proxy to reconstruct past UV-B changes is very exciting. It is so cool to get the opportunity to work with such inspiring and excellent researchers as you are. The support and attention you have given me these past six months has been amazing, thank you so much for helping me reach the finish line.

I am also really grateful for been given the opportunity to work alongside Alistair Seddon. He is an outstanding young researcher with a good eye for details which has been very important to successfully establish the py-GC/MS method in Bergen. I have learned so much from you during these past three years, and I believe we have been a great team. I think of you as my "science big Brother" and I hope we can work together in the future.

In the Parasol project I also had the pleasure to learn from and work with Tanja Barth, H. John B. Birks and Anne B. Bjune, thank you for your input, discussions and encouragement, particularly during these past months. It was a welcome relief when Linn C. Krüger helped me out with picking pollen samples during the last year of my PhD. In addition, I want to thank Amy Eycott, Joanne Inchbald and Tessa Bargmann for proof reading my thesis and Joseph Chipperfield and Richard Telford for spontaneous stats meetings and discussions.

The EECRG is a great research group to be part of and with weekly meetings where we can present and listen to ideas, progress, results, and have fruitful discussions is both inspiring and educational. I think our social dynamic is unique and I want to thank you all for a good place to work, Friday board game nights were a lot of fun.

There were some people who were always there for me when I struggled the most, and I am ever grateful for your support and encouragement. Thank you so much for being there; Eirik, Marianne, Lise, Vivian, Tessa, Christine, and especially Aud!

Finally, I wish to thank my family. My grandmother always valued education is highly and I think she would have been very proud now. My mother and father founded my love for nature and I am so grateful for your eternal support, advice and love.

Everyone who goes down the PhD road to become a scientist knows that at some point you will run into difficulties This could be related to field work, experiments, statistical analyses, supervisor issues, or simply a moody Georg Constanza (our GC machine). For one and a half years he pretended to work for a few weeks, just to show us that in actual fact, we did not get reproducible results after all. Because every time we thought we had solved the problem, a new one arose. Without Alistair's stamina and meticulous approach to the issues we encountered, we would not be getting as reliable results as we are now.

In the PARASOL project we have picked 1 284 pollen samples and a total of 253 500 pollen grains. We have run more than 2 100 analyses with the THM py-GC/MS method which equals 263 working days in the lab. I ran my last sample in late July 2016.

This PhD has been funded by the Norwegian Research Council FRIMEDBIO programme (Project number 214359) and additional support was given by the Olaf Grolle Olsens legat. The four-month extension (including three weeks of field course teaching) given by the Department of Biology, UIB was essential to complete this thesis. I want to thank the people in our department and Tommy Strand for being encouraging and helpful during these past months.

List of Papers

This thesis is based on the three following papers and one appendix:

Paper I: Alistair W. R. Seddon, Mari Jokerud, Tanja Barth, H. John B. Birks, Vigdis Vandvik and Kathy J. Willis. An adapted protocol for reconstructions of surface UV-B radiation using thermally assisted hydrolysis and methylation of *Pinus sylvestris* pollen. Submitted to *Review of Palaeobotany & Palynology*.

Paper II: Mari Jokerud, Alistair W.R. Seddon, Joseph Chipperfield, Kathy J. Willis and Vigdis Vandvik. Plastic responses and species-level variation of UV-B absorbing compounds in *Pinus* spp. to short-term variation in UV-B radiation. Submitted to *New Phytologist*.

Paper III: Mari Jokerud, Alistair W.R. Seddon, Tanja Barth, Anne E. Bjune, John B. Birks, Kathy J. Willis and Vigdis Vandvik. Pollen chemistry and UV-B radiation: Determining the temporal window of response in *Pinus sylvestris* along a latitudinal gradient in Europe. Submitted to *Proceedings of the Royal Society B*.

Declaration

Tasks	Paper I	Paper II	Paper III	Appendix
Paper idea	AWRS, **MJ**, TB	VV, **MJ**, AWRS	**MJ**, AWRS, VV, KJW, HJBB	
Project design	KJW, VV	KJW, VV	KJW, VV	
Study design	AWRS, **MJ**, TB, VV, KJW, HJBB	**MJ**, AWRS, VV	**MJ**, AWRS, VV, KJW, HJBB	
Field work (Europe)		**MJ**	**MJ**	
Field work (Norway)	AWRS, **MJ**	**MJ**, AWRS	**MJ**, AWRS	
Pollen picking	**MJ**, AWRS, LCK	**MJ**, LCK	**MJ**, LCK	
Statistical analyses	AWRS	**MJ***, AWRS*	**MJ***, AWRS*	
Writing	AWRS	**MJ**, AWRS†, JDC‡	**MJ**	**MJ**, AWRS†, JDC‡
Text editing	**MJ**, TB	VV, AWRS	AWRS, VV	
Comments and other inputs	VV, KJW	KJW, JDC, HJBB	AB, HJBB, TB, VV, AWRS	

MJ = Mari Jokerud, AEB = Anne Elisabeth Bjune, AWRS = Alistair Seddon, HJBB = H. John B. Birks, JC = Joseph Daniel Chipperfield, KJW = Kathy Jane Willis, LCK = Linn Cecilie Krüger, TB = Tanja Barth and VV = Vigdis Vandvik. Within each list, authors are listed in order of decreasing contribution.

*The Bayesian model was written independently by both authors, and later merged for the analyses.

†AWRS wrote the paragraph on Bayesian hierarchical modelling and the modified protocol for THM-py-GC/MS of Pinus sylvestris pollen.

‡JDC wrote the mathematical expressions of the Bayesian hierarchical modelling.

Introduction

The total amount of ultraviolet radiation (UV-B wavelength = 280–315 nm) reaching the Earth' surface has probably experienced large changes throughout Earth's history. Evidence suggests that during some periods, some regions received up 60-80% higher UV-B radiation than in the present (Beerling et al., 2007, Willis et al., 2009). High UV-B flux rates have potentially major consequences for biodiversity and ecosystem functioning; affecting all aspects of ecosystems from biomes through to genes, including altering the mode and tempo of evolution (Shaffer and Cerveny, 2004, Willis et al., 2009). An important, yet untested hypothesis, is that past variations in UV-B flux have had a significant impact on the tempo and mode of speciation and extinctions, which in turn may be mirrored in global biodiversity patterns (Willis et al., 2009). To address this hypothesis many questions remain to be answered. For example, during intervals of enhanced UV-B radiation, is there evidence for mutant forms of plant and animal life, greater turnover in populations, and more/less speciations than extinctions? Across what spatial scales is this apparent? Are such changes more frequent in regions with less cloud cover or at higher altitude? The first step in addressing such questions, however, is to devise a method to measure surface UV-B through time; this can then be used as a baseline against which to measure fossil and molecular records, recording for example, changing species distributions, community composition, nutrient cycling, lineage splits and speciation rates.

Current and past variation in UV-B flux is affected by different sources, including orbital variations, ozone depletion, volcanism and cloudiness (Shaffer and Cerveny, 2004, Visscher et al., 2004, Beerling et al., 2007, Bjorn and McKenzie, 2007, Herman, 2010). Up until now, it has not been possible to reconstruct an accurate measure of UV-B flux through time. A newly-developed thermally assisted hydrolysis and methylation pyrolysis-gas chromatography and mass spectrometry method (THM py-GC/MS) measures UV-B absorbing compounds in both extant and fossil pollen and spores (Blokker et al., 2006, Blokker et al., 2005, Rozema et al., 2009). Willis et al. (2011) demonstrated a relationship between quantitatively measured *p*-Coumaric acid in *Pinus spp.* along a UV-B radiation gradient across Europe and were the first to successfully

reconstruct UV-B flux through the Holocene using *Pinus* fossil pollen and the *py*-GC/MS method.

Effect of UV-B radiation on plants

Elevated UV-B radiation is correlated with DNA damage in plant foliage and errors in DNA repair, leading to an increased probability of genome instability, a higher risk for replication errors, and the transfer of toxic and mutagenic effects to ensuing generations (Caldwell et al., 2003, Caldwell et al., 2007, Willis et al., 2011). Numerous studies have investigated the effects of UV radiation on biodiversity and ecosystems in deep time, however, there is very little knowledge about how UV-B fluxes have changed through time and the effects on biodiversity and ecosystems. Nevertheless, this is an issue of great interest to a wide range of scientists, including geophysicists, climatologists, ecologists and biologists, and their 'palaeo' colleagues (Willis et al., 2009). Molecular phylogenetic studies found evidence for radiation and diversification of species which are endemic to the Qinghai-Tibetan Plateau (*Ligularia, Cremaenthodium, Parasenecio* and *Saussurea*) between 20 and 7 Myr. This diversification coincides with the major uplift of the Q-T plateau since the early Miocene (Liu et al., 2006, Wang et al., 2005). Willis et al. (2009) calculated a possible enhancement of UV-B radiation of approximately 100 % during the past 50 Myr at the Q-T plateau, and propose that the increase of UV-B radiation could have caused mutagenesis and change in growth responses, thereby leading to speciation. Mutagenesis in terrestrial plants is apparent by the occurrence of abnormal spores and pollen at the end of the Permian (251 Myr), and is attributed to a hypothesised enhanced UV radiation which was a consequence of the eruption of the Siberian Traps, and the global collapse of the stratospheric ozone layer (Beerling et al., 2007, Foster and Afonin, 2005, Visscher et al., 2004). Rates of diversification through time have frequently been acknowledged to be linked to variations in UV-B flux (Lee and Lowry, 1980, Davies et al., 2004, Visscher et al., 2004, Clarke and Gaston, 2006, Beerling et al., 2007, Bjorn and McKenzie, 2007, Flenley, 2007, Willis et al., 2009).

The effects of elevated UV-B radiation on plants are reductions in growth rate, plant height, foliage area, leaf area and decreased shoot mass (Newsham and Robinson, 2009,

Li et al., 2010, Rozema et al., 1997, Ballare et al., 2011). Tropical 'dwarf forest' which dominates the forest line in mountains around the Equator, shows stunted tree growth: leaves are small, thick and coriaceous with a hypodermis, and extra pigments also present (Flenley, 2007). Flenley (2007) propose that this forest type represents the physiological responses of plants grown under high levels of UV-B through time and Li et al. (2010) show that woody perennials are less sensitive to UV-B radiation than herbaceous plants.

Research shows that the production of UV-B absorbing compounds, such as phenolic acids (e.g. Ferulic and *para*-Coumaric acid) increase in response to exposure to UV-B (Rozema et al., 2001b, Rozema et al., 2002, Fraser et al., 2011, Searles et al., 2001). Phenolic acids are considered to be part of the defence system of plants, protecting them against harmful UV-B radiation (Blokker et al., 2006, Treutter, 2006, Willis et al., 2011). Phenolic acids act as effective sunscreens as they absorb and scatter the energy associated with ultraviolet radiation (Wehling et al., 1989, Rozema et al., 2001b). It is suggested that these responses to enhanced UV-B are a result of change in energy allocation from growth to protection (Ballare et al., 2011, Zavala and Ravetta, 2002).

Alteration of plant tissue chemistry such as, UV-B-induced phenolic acids is also related to cross-tolerance with other environmental stressors (Ballare et al., 2011). Phenolic acids are linked with direct defence against herbivores as these compounds have common signalling pathways and may have toxic effects on plant consumers (Ballare et al., 2011, Demkura et al., 2010). This can affect the choice of sites for insect feeding and egg-laying in addition to insect growth and survival. Studies also show an increase herbivory under decreased UV-B radiation conditions (Ballare et al., 2001, Caldwell et al., 2007). These combined effects along with a decrease in plant biomass, morphological and DNA changes (Ballare et al., 2011, Llorens et al., 2015, Bornman et al., 2015), can have knock-on effects by affecting the competitive ability of plants, and may lead to changes in ecosystem structure and processes.

Reconstructing past UV-B changes using biological proxies

To measure changes in the chemistry of sporopollenin, two approaches can be used. Fourier transform infrared microspectroscopy (FTIR) is relatively quick and can be used on a small number of grains (Fraser et al., 2012, Jardine et al., 2015, Lomax et al., 2008). This method has therefore been proposed as a tool to reconstruct past UV-B. In FTIR, the sample is irradiated by a polychromatic light and a movable mirror produces a time dependent signal that is transformed by Fourier transformation into a frequency spectrum. The light excites the atoms in a sample and causes movements referred to as vibrations. Stretch vibration changes the bond lengths in a molecule, either symmetrically or asymmetrically, and bending vibration changes the angles of the bond in a molecule (Stuart, 2004). The position of the absorbance band identifies the type of bond/ functional group present, whilst variations in band height and area represent changes in relative abundance of such bonds/ groups (Fraser et al., 2011). The aromatic ring structure of both *para*-Coumaric and Ferulic acid has a distinct vibrational frequency detectable by FT-IR microspectroscopy (Lomax et al., 2008). Promising work has been conducted by Fraser et al. (2011), Lomax et al. (2008), Jardine et al. (2015) and others. However, FTIR has the disadvantage of only providing relative abundances after standardisation to the relatively more stable groups (OH) found within the chemical spectra. Also, it is more difficult to resolve individual components of sporopollenin, e.g. separate Ferulic and *para*-Coumaric acid.

On the other hand, thermally assisted methylation (THM) reaction with pyrolysis gas chromatography mass spectrometry (py-GC/MS) measures quantitatively the amount of *para*-Coumaric and Ferulic acid. Further development, i.e. to improve sample reproducibility of the THM py-GC/MS method based on previous work by Blokker et al. (2005), Willis et al. (2011) is essential for the utilisation of the method. This may enable quantification and reduced uncertainties of the THM py-GC/MS method, ensuring a more precise quantitative measurement of *para*-Coumaric and Ferulic acid in *Pinus* spp. pollen. THM involves using a strong base reagent (tetraammonium hydroxide, TMAH) to depolymerise the constituents within the sporopollenin and subsequently convert them to methyl-esters. The TMAH reacts with the macromolecule in a directed manner to increase the yield of the analyte and decrease secondary pyrolysis

reactions (Blokker et al., 2005). The derivatives that result are chemically stable and thus more readily quantified with py-GC/MS.

Py-GC/MS is an instrumental technique that enables a reproducible characterisation of the intractable and involatile macromolecular complexes found in virtually all materials in the natural ecosystem. In py-GC/MS, the sample is exposed to high temperatures in an oxygen free environment at a pre-set temperature for a number of seconds within a pyrolysis unit, generating small volatile fragments (Wampler, 2006). The mixture of compounds is then transferred into the analytical column of a gas chromatography machine, and the different molecules have different retention times depending on size, shape and polarity.

Phenolic acids in pollen

Ferulic and *p*-Coumaric acid in spores and pollen can screen out more than 80% of the incoming UV-B radiation (Rozema et al., 2001a). These compounds are thought to be the building-blocks of sporopollenin, the major biomolecule that constitutes the pollen exine (Wehling et al., 1989, Rozema et al., 2001a, Blokker et al., 2006, Jungfermann et al., 1997). The link between phenolic acids and UV-B radiation has recently been established, see Blokker et al. (2006), Blokker et al. (2005), Rozema et al. (2001b), Lomax et al. (2008), Fraser et al. (2011). The pollen chemical record is preserved in sediments because sporopollenin (*p*CA) is highly resistant to degradation under anoxic conditions. As *Pinus* spp. pollen is produced in vast quantities in addition to being relatively large and having a long fossil history, pine species have been proposed as a UV-B proxy for centennial timescales or longer (Willis et al., 2009, Willis et al., 2011, Lomax and Fraser, 2015).

A general dose-response relationship between solar UV-B and phenolic acids has been established through both field and experimental research, for example in *Vicia faba* pollen grown under different UV-B radiation intensities (Blokker et al., 2005, Rozema et al., 2001a), in *Pinus* species pollen grains along a UV-B gradient across Europe (Willis et al., 2011) and in *Lycopodium annotinum* spores and degree of shading under birch canopies (Fraser et al., 2011). As mentioned earlier, Rozema et al. (2001b)

suggests that aromatic compounds are produced as a defence response to UV-B radiation during the growing season in order to reduce UV-B induced DNA damage and mutagenesis, which can be potentially harmful or lethal to the DNA (Rozema et al., 1997, Tuteja et al., 2001). Lomax et al. (2008) also revealed a correlation between phenolic concentrations in *Lycopodium annotinum* spores and changes in UV-B radiation during the growing season over a 30-year period. However, this short-term assertion has not been explicitly tested under field conditions (Rozema et al., 2009) and the eco-physiological response that results in the production of phenolic compounds in pollen remains poorly understood.

Pollen development and tapetal cells

According to Owens (2006), the reproductive cycle of *Pinus contorta* Dougl. is similar to most other *Pinus* spp. and the pollen cone cycle extends over about 12 months. The development of pollen buds initiates the year prior to pollen dehiscence and begins with long shoot bud development (LSB) where small scale like leaves (cataphylls) start growing in March/April (Fig. 1 i). In May, an axillary bud is initiated above these cataphylls, which then develops into four types of buds: pollen buds, short shoot buds, seed cone buds or LSB, where the latter develop into lateral branches (Fig. 1 i). The pollen bud usually differentiates in July/August initiating the production of microsporophyll primordia. Development of these cells continues until about 140 microsporophylls containing two microsporangia each, have formed by the end of September. After this period of initial development the pollen bud then goes into winter dormancy (Fig. 1a) (Owens, 2006, Owens and Molder, 1977).

In mid-March in the year of dehiscence the pollen cone bud resumes development and undergoes cell division into 500 micro-sporocytes. This is followed by meiosis, where the chromosomes replicate once but the cells divide twice, resulting in four haploid microspores containing 12 chromosomes. These four microspores are named a tetrad, and the tetrad is held together for just a few days before the micro-sporophyte bursts and releases over 2000 microspores into the thecal fluid within each microsporangium (Fig. 1 c). The complete meiosis process and formation of separate microspores takes approximately 2 weeks (Owens, 2006).

During the next month, microspores develop into mature pollen grains and, in the first week of pollen maturation, the microspores become rounded and store food reserves (mostly consisting of starch), and the exine wall thickens and starts to form two small sacci (Fig. 1 d). Mitosis starts about three weeks after meiosis and during this period the intine is created next to the exine (Fig. 1 e). Then the central cell forms a large antheridial cell (Fig. 1 f, g) which later divides into two cells; a sterile cell (stalk cell) which has no further function, and a generative cell that divides to form sperm after pollination (Fig. 1 h) (Owens, 2006). In these final stages before dehiscence (Fig 1 g, h), the tapetal cells produce a peritapetal membrane containing sporopollenin (including *p*CA) that cover the exine of each pollen grain (Dickinson, 1970, Dickinson and Bell, 1976, Dickinson and Bell, 1972, Rowley et al., 2000). In *Pinus sylvestris*, the peritapetal membrane is produced fewer than 11 days prior to pollen shed and the tapetal cells degenerate the same day or up to two days before dehiscence (Rowley et al., 2000). As a result, even shorter-term plastic responses may be possible compared with those proposed by Rozema et al. (2001b).

In summary, given what we know about pollen development and the formation of *p*CA from eco-physiological research in *Pinus* spp., determining the timing and extent of this plastic response remains an essential question in understanding how species respond to changes in UV-B radiation. Although Willis et al. (2011) were the first to establish a relationship between spatial variation in mean long-term UVB and abundance of sporopollenin-based *p*CA, whether the signal represents a short-term flowering season or longer-term growing season response remains unknown. Furthermore, the extent to which the effects are experienced locally in the plant (i.e. if variability is observed within a tree shaded in different ways or if the signal represents a fully-integrated tree response) remains an open question.

The importance of understanding species effects

Another neglected component in work on a pollen-based UV-B proxy so far is the variation in both the *p*CA content and in the response to environmental variation between different species. Pollen from members of the European flora of *Pinus* spp.

remain difficult to separate using traditional, light microscopic methods. If different species exhibit varying UV-B responses under equivalent UV-B radiation, and respond differently to variation in UV-B radiation, then this could have implications for both dose-response relationship of *p*CA abundance and reconstructions from pollen sampled

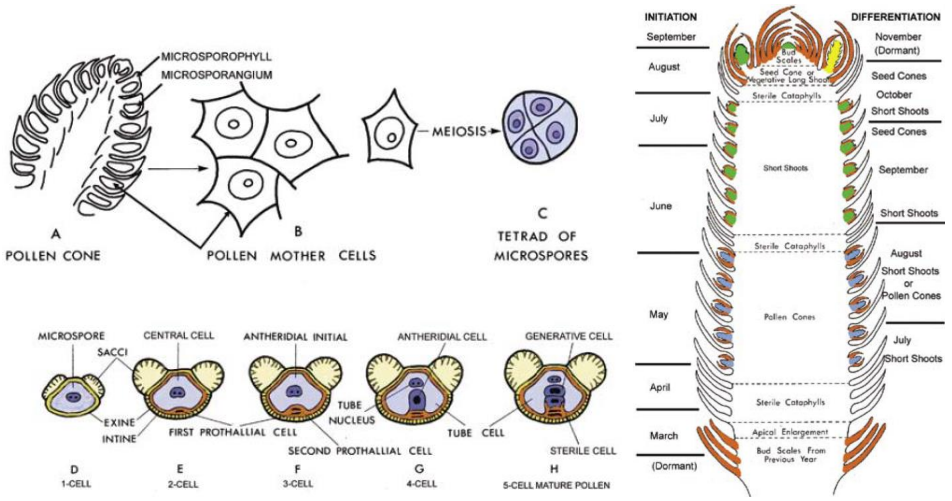

Figure 1. a) Pollen development in pine. Haploid (N) gametophytic cells are shown in blue, the outer (exine) layer of the pollen wall is shown in yellow and the inner (intine) layer of the pollen wall is orange. **i)** Diagram of a long shoot bud showing the time of initiation of axillary buds and the approximate time of differentiation of these buds. Green indicates vegetative terminal and lateral long-shoot or short-shoot buds or apices, yellow indicated a seed-cone bud and blue indicate pollen-cone buds. Brown indicates the bud scales. Reprint: Owens JN 2006. The reproductive biology of lodgepole pine: Forest Genetics Council of British Columbia. FGC extension note; 07.

from a sediment core. An obvious source of species-level variation in UV-B absorbing compounds may be pollen size. European *Pinus* spp. vary considerably in pollen size (Beug, 1961), and it is very likely that species may contain differences in total *p*CA simply due to mass difference. In palaeoecological reconstructions, such variation can be accounted for simply by measuring and taking into account average pollen size. Species-level variation in *p*CA abundance due to inherited genetic differences in the ability to produce these acids, or in the response to variation in UV-B radiation, is more challenging for palaeoecological reconstructions. The extent to which species-level variation can potentially affect both the dose-response relationship between *p*CA and UV-B radiation and the reliability of reconstructions of past UV-B flux remains poorly understood.

Objectives

This thesis encompasses two main objectives: 1) methodological improvement of the thermally assisted hydrolysis and methylation pyrolysis-gas chromatography and mass spectrometry method by Blokker et al. (2005), Willis et al. (2011) and 2) examination of the eco-physiological response of UV-B absorbing compounds and effects of UV-B radiation on *Pinus* species. Here are the following aims:

1. Modify, test and validate the THM py-GC/MS method.
    a. In order to improve sample reproducibility, we investigated whether introducing an internal standard (Nonadecanoic acid; NAA) would enhance the analytical precision of the THM py-GC/MS method. We hypothesise that this will enable us to quantify and reduce uncertainties of this method and to ensure a more precise quantitative measurement of *p*CA ratio in *Pinus* spp. pollen.
    b. In order to determine sample sizes and experimental setup for *Pinus* spp., we investigated the relationship between number of grains and *p*CA ratio, and the signal-to-noise ratio (**Paper I**).

2. Examine the eco-physiological response of UV-B absorbing compounds to UV-B flux.
    a. In order to investigate whether *Pinus* spp. displays a plastic response to short-term changes in UV-B radiation we designed two experiments (**Paper II**):
        i. Our first experiment was designed to investigate the effect of short-term reduction (one month) in UV-B radiation during the pollen development period of *Pinus sylvestris*.
        ii. Our second experiment was designed to test the effect of *p*CA abundance between two years with natural variation in UV-B on the same trees of several *Pinus* spp. We expected these experiments to give insights into the short-term plasticity effect of UV-B, at the flower or pollen level in *Pinus sylvestris*.
    b. In order to examine the timing of the response of *p*CA in *Pinus sylvestris* we explored the relationship between *p*CA abundance and different UV-B periods across Europe within the same year. (**Paper III**).

c. In order to investigate the importance of species-level variation, we compared *p*CA abundance in the same trees of four different *Pinus* species in two consecutive years with natural variation in UV-B radiation. (**Paper II**).

Material

Study species

Native European *Pinus* species and in particular *Pinus sylvestris* were chosen as proxy species in this thesis. *Pinus sylvestris* is the most widespread of the European species in the genus and its natural distribution ranges across large areas of Europe and to East-Russia (Fig. 2) (Debreczy et al., 2011). It is a light-demanding species and as previously mentioned, *Pinus* spp. pollen is produced in vast quantities, and the pollen grains are relatively large and have a long fossil history.

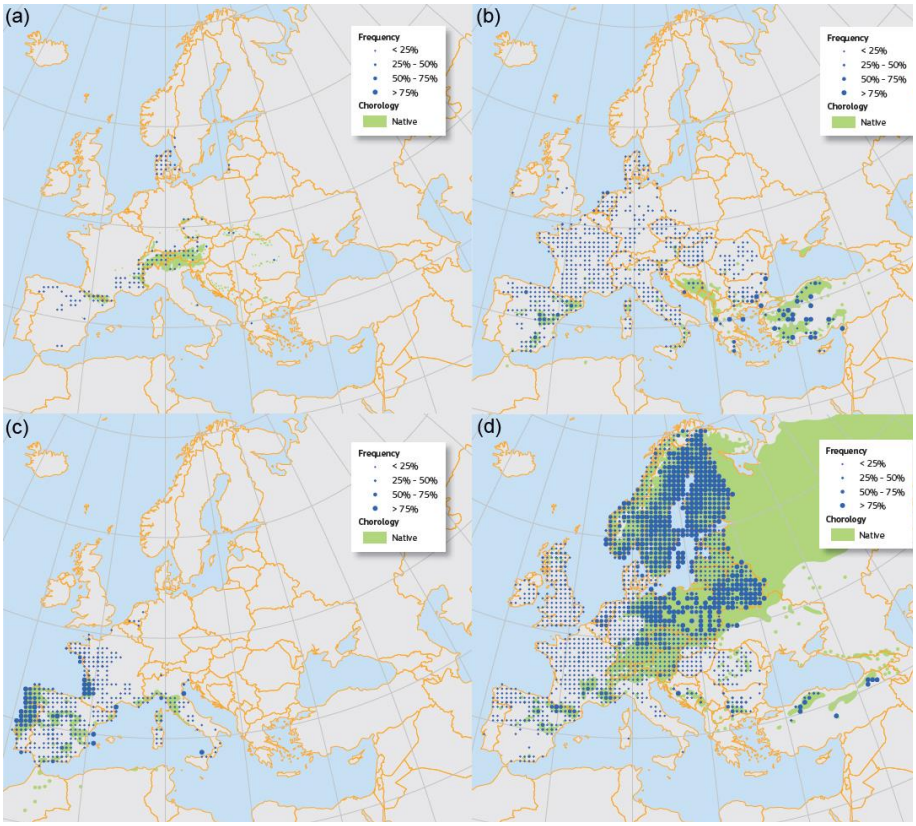

Figure 2. Distribution maps of some of the native European *Pinus* species from The European Atlas of Forest Tree Species. **a)** *Pinus mugo*, reprint from Ballian et al. (2016), **b)** *Pinus nigra*, reprint from Enescu et al. (2016), **c)** *Pinus pinaster*, reprint from Abad Viñas et al. (2016) and **d)** *Pinus sylvestris*, reprint from Houston Durrant et al. (2016).

Sampling areas and laboratory analyses

Paper I

In order to improve sample reproducibility, we investigated whether introducing an internal standard (NAA) would enhance the analytical precision of the THM py-GC/MS method. This was done by preparing five calibration solutions containing ratios of approximately 1:1, 1:1.25, 1:1.5, 1:1.75 and 1:2 concentrations of NAA (~0.01g) and *p*CA (~0.01 g, 0.0125 g, 0.015 g, 0.0175 g, 0.02 g) respectively, dissolved in 0.4 ml of MEOH and 0.2 ml of 25% TMAH (in MEOH) and made up to 1 ml with MEOH. The standards were stored at 4°C in between sample analysis. 1 µl of solution was applied to the inside of the microvial using a 1µl SGE syringe with a 50mm Needle and Pt#1 tip (509221).

In this paper we used sun-exposed *Pinus sylvestris* pollen samples from the Arboretum and Botanical Garden at Milde in Bergen (N 60.2557, E 5.2706). We ran 3 replicates of 200 grains per sample so that the full derivatives of the THM reaction from the pollen could be established. To investigate whether NAA is naturally present in the derivatives from a pollen sample we ran one sample adding 50 µl of an internal NAA standard solution (0.001 g NAA dissolved in 1 ml MEOH) to the TMAH solution. To test the relationship between number of grains and both *p*CA abundance and signal-to-noise ratio of the machine we prepared samples containing between 50 and 400 grains.

Paper II

To investigate short-term plasticity in *Pinus* spp. we designed a shading experiment in which ten freestanding/sun-exposed *Pinus sylvestris* trees 6–8 metres in height were selected from the Arboretum and Botanical Garden at Milde in Bergen, Norway (Fig. 3). Two branches on each tree were used, one randomly allocated to the shade treatment and covered with a shade cloth fabric with 90% shade intensity, the other marked and left without any shade cloth under ambient UV-B radiation. The experiment was initiated on April 28th 2014 and pollen was collected on May 28th 2014 (**Paper I, II**). We analysed 60 samples; ten trees, two treatments and three replicates.

To investigate responses of short-term natural variation in UV-B between years and species-level variation in the response, we collected pollen samples in 2013 (collection date: May 13th) and 2014 (May 26th) from the same *Pinus cembra* L.*, P. mugo* Turra*, P. nigra* J.F. Arnold*, P. peuce* Griseb.*, P. pinaster* Aiton*, P. sylvestris* L. and *P. uncinata* Ramond ex DC. trees in both years in Geneva Botanical Garden and Conservatory (N 46.2253, E 6.1465). We analysed one to three trees per species and three replicates per tree, resulting in 73 analysed samples. *Pinus cembra, P. nigra, P. pinaster and P. uncinata* samples contained 150 pollen grains, but due to the smaller pollen size and in order to avoid *py*-GC/MS results close to the machine detection level, samples of *Pinus mugo* and *P. sylvestris* contained 200 pollen grains. In **Paper II,** 133 samples were analysed for *p*CA.

Paper III

To investigate the timing of the response we collected *Pinus* spp. pollen samples from 21 arboreta/botanical gardens across Europe in 2014. Due to time constraints we chose to investigate the timing of the response in *Pinus sylvestris* pollen samples from 13 arboreta/botanical gardens during dehiscence season from the 7th of April 2014 until the 8th of June 2014 across Europe covering Southern Norway (60.25 N) to Southern Spain (37.87 N). A complete list of arboreta is found in Appendix, Table A1 (Fig. 4). We received pollen samples of *Pinus sylvestris* from the Cordoba Arboretum, however since the only tree of *Pinus sylvestris* observed during collection was young and surrounded by fully-grown trees, these samples were not used in our analysis. We analysed 68 samples of *Pinus sylvestris* across Europe for *p*CA. The arboreta in Bergen and Geneva contain ten and six trees, respectively, while the 11 other arboreta contain one tree. We ran three replicates per tree.

For sample preparation and details on chemical analysis and settings, see Appendix (A3, A4 and A5). In **Paper I**, we ran the analytical solutions and *Pinus sylvestris* in full scan mode so that the full derivatives of the THM reaction could be established, while the number of pollen grains test was run in selective ion monitoring (SIM). In **Paper II** and **III**, the mass spectrometer was run in SIM mode to increase detection of *p*CA and NAA.

In all locations we sampled each tree during or immediately before dehiscence; one male pollen bud (flower) from each of five branches was collected per tree, and each male pollen bud was placed in its own paper bag within a plastic zip lock bag to minimize contamination (Fig. 3). Samples were stored at room temperature in sealed plastic boxes.

Figure 3. Field work photos. Top left: Alistair Seddon is placing a shade cloth on *Pinus sylvestris*. Top middle: Collected samples of extant *Pinus* spp. pollen and needles. Top right: *Pinus pinea* in the Botanical Garden of Barcelona. Middle left: Immature pollen of *Pinus sylvestris* from The Lourizán Botanical Garden in Pontevedra. Bottom left: *Pinus pinaster* from the botanical garden of Cordoba. Bottom right: The author collecting pollen with telescope garden scissor in the botanical garden of Athens.

Statistical analyses

Estimated dehiscence date

In **Paper III** we estimated dehiscence date using the European daily high-resolution gridded data set of surface temperature and precipitation for 1950–2006 (E-OBS) (Haylock et al., 2008) and modified the heat sum method for *Pinus banksiana* Lamb. to calculate the maximal pollen release date from Di-Giovanni et al. (1996) This was done because pollen collection in some arboreta did not occur at the exact date of dehiscence, due to practical limitations. We set the January-February 2014 mean temperature as the initiation temperature, unless this temperature was lower than 4°C, in which case the initiation temperature was set to 4°C. The first day in 2014 with temperature above the initiation temperature was used as start date and we then estimated dehiscence date as the date when the sum of daily mean temperatures from the initiation temperature reached 288.58 degree days (Di-Giovanni et al., 1996). Field notes on pollen maturity were used to verify dehiscence date.

Current UV-B data

In **Paper II** and **Paper III** incoming UV-B radiation (J m^2) data for arboreta were obtained from the Spectral Surface UV-B Radiation and erythemal dose level-3 data product (Kalakoski, 2012) provided by NASA Goddard Earth Sciences Data and Information Services Center (GES DISC) using the Mirador interface (http://mirador.gsfc.nasa.gov/cgi-bin/mirador/collectionlist.pl?keyword=omuvbd).
Resolution of this data product is a 0.25° by 0.25° grid in longitude and latitude and a correction has been applied to account for clouds, scattering aerosols and absorbing aerosols (Tanskanen et al., 2007, Arola et al., 2009). We used daily UV-B erythemally weighted daily dose (J m^2) data from January 1st 2005 to December 31th 2015. **In Paper II**, the daily measurements were summarised into monthly mean UV-B erythemal dose values and averaged across all years to calculate monthly anomalies (Fig. 5). **In Paper III**, the daily measurements were summarized into mean UV-B erythemal dose for different potentially important time periods: (i) the pollen development season, where a total of twelve different durations were tested from one week (7 days) to twelve weeks (84 days) prior to estimated dehiscence date, (ii) during pollen bud growing season (July

– October 2013) and (iii) long-term mean (January 1st 2005 to December 31th 2015) for each arboretum, see Paper III.

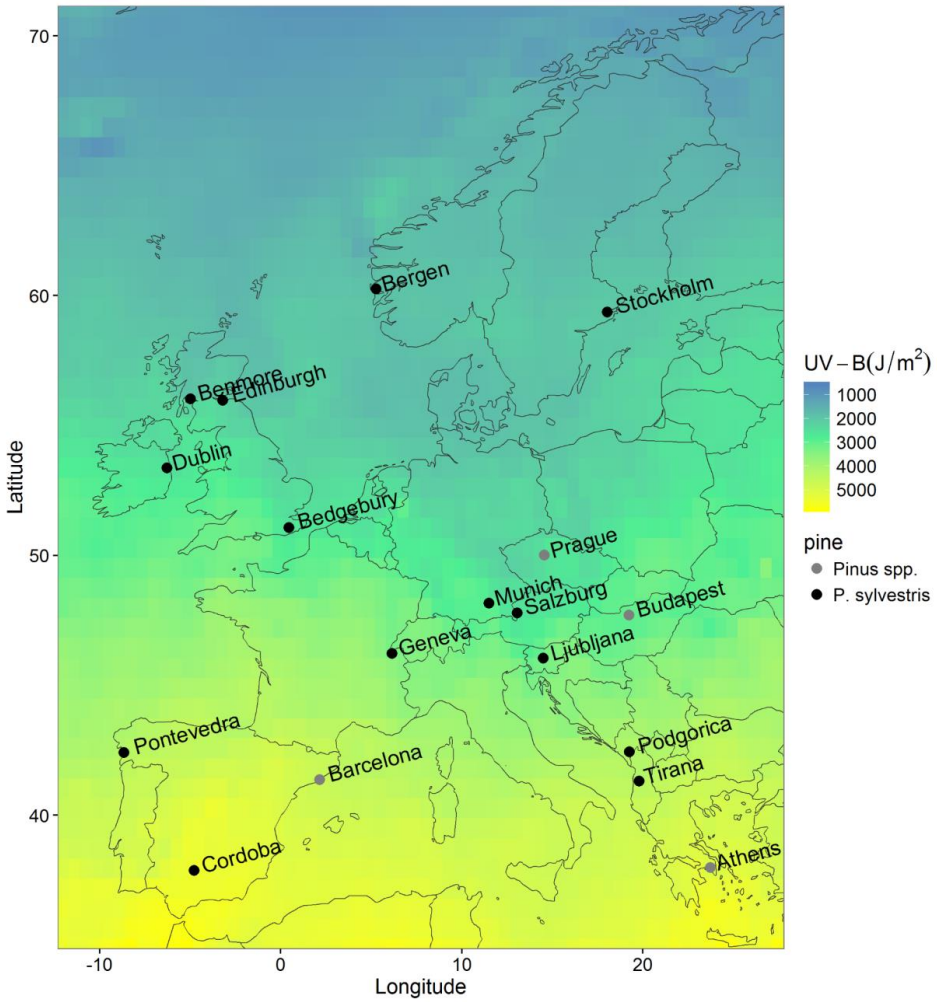

Figure 4. Average UV-B radiation across Europe in April-May 2014, including the locations of the arboreta for collection of extant *Pinus sylvestris* (in black) and *Pinus* spp. (in grey) pollen.

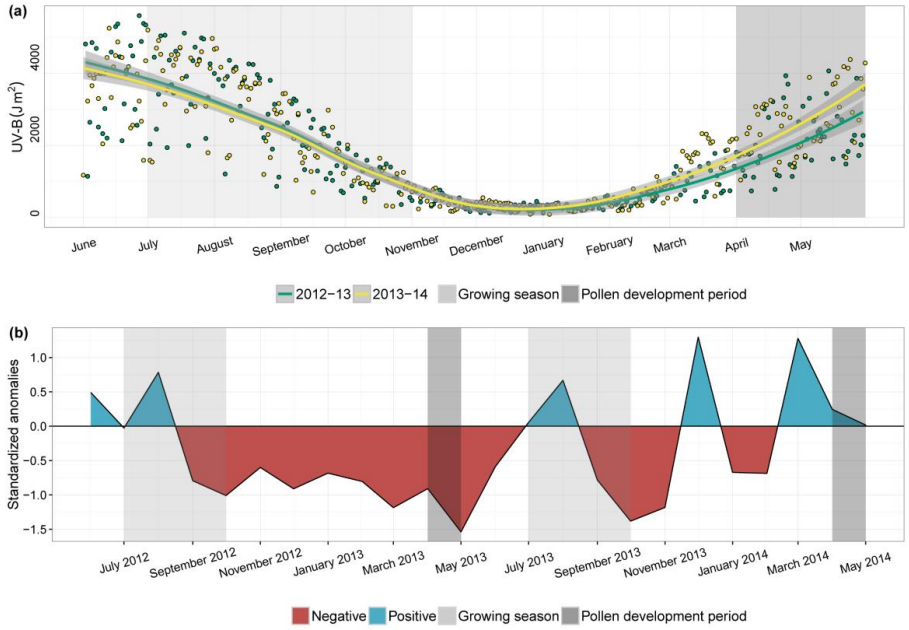

Figure 5. a) Daily UV-B radiation in Geneva: green is time period June 2012-2013 and yellow is June 2013-2014, both are fitted with a loess smoothed line with a 95% confidence interval. **b)** Monthly standardized anomalies in Geneva: red areas are negative and blue areas are positive anomalies. Pollen season (dark grey area) is the pollen development which occur two months prior to dehiscence (April-May) and growing season (light grey area) is male pollen cone bud growth (July-October).

Paper I

Peak heights were detected using the MALDIquant package (Gibb and Strimmer, 2012) in R (version 3.2.1) (R Core Team, 2016). Before quantifying peak heights, a baseline correction procedure was used following a Statistics-Sensitive Non-Linear Iterative Peak-Clipping algorithm (Ryan et al., 1988), and the background-noise level was estimated by finding the median absolute deviation. Relative standard deviation (RSD) was calculated to assess the analytical precision of *p*CA ions (m/z 161 and 192) and NAA ions (m/z 74, 87 and 312). A linear regression model was used to analyse the relationship between i) analytical *p*CA (m/z 161) and internal standard (NAA: m/z 74) and ii) *p*CA ratio and the number of grains added to the sample. Signal-to-noise ratios at different numbers of pollen grains were calculated by dividing the m/z 161 peak

height with 2 times the median absolute deviation of the estimated background noise level on square-root transformed data. Linear and sigmoidal models were fitted to the m/z 161: 74 ion ratios and the m/z 161 ion signal-to-noise ratio against the number of grains using non-linear least squares in the nlme package (Pinheiro et al., 2013). In our tests, the initial sample at 200 grains was found to have anomalously low values of pCA so we reran this sample and report the mean value of the two samples here.

Based on our results in **Paper I**, we applied the *p*CA ratio in our statistical analyses in **Paper II** and **III**. We used measurements in pollen size by Beug (1961) to estimate pollen surface area in order to account for differences in pollen-grain size among the species collected in Geneva (**Paper II**).

Bayesian hierarchical models

There is a new wave in palaeo inference using Bayesian models (Salonen et al., 2012, Dawson et al., 2016, Holden et al., 2016). We developed a hierarchical model to test our different hypotheses, inspired by Jackson (2012)'s emphasis on incorporating uncertainties to strengthen palaeoecological inference. Our statistical Bayesian frame work is novel because it allows us to characterise experimental and analytical uncertainties more appropriately than in a frequentist model. By incorporating these uncertainties we are able to estimate more realistic *p*CA values. This framework will provide a statistical basis for future palaeoecological reconstructions of UV-B, for example age-depth and pollen dispersal models can be incorporated into the model.
There are two terms which need to be understood, the first being the priors. We built two models which incorporate information on pollen picking precision and analytical precision. The pollen picking precision prior model is based on a pollen picking test where we picked 50 pollen grains and recounted the actual number of pollen being picked. This was repeated 30 times. In the prior model of analytical precision we used the *p*CA:NAA ratio from the calibration solutions. The information from these tests were applied to the informative priors so their likelihood was more constrained in our hierarchical model.

The second term is the likelihood (the model) which describes the information that we get from the set of measurements. The likelihood consists of several sub models. The Markov Chain Monte Carlo (MCMC) simulation draws the probability of the *p*CA measurement from the prior distribution of the number of pollen grains and analytical precision. The posterior estimates can then be introduced in the form of a probability distribution with credible intervals which represent the likelihood that any one sample has a particular *p*CA measurement.

We used a hierarchical model in **Paper II** to test for differences in i) *p*CA quantity between shaded and sun-exposed pollen of *Pinus sylvestris*, ii) *p*CA quantity between pollen produced in 2013 and 2014 and iii) variability of *p*CA in different *Pinus* species under equal UVB-influx conditions. **In Paper III** we used a Bayesian hierarchical model to test different UV-B radiation periods against *pCA* ratios along an UV-B gradient across Europe. Parameters of the model were estimated using Bayesian inference. The model (likelihood) was designed to characterise uncertainty at different stages of the analytical process, and was based on three main components. For further statistical information, see Appendix, A2.

Our models in **Paper II** were specified in JAGS (Plummer, 2016a), using an adaptation phase of 10 000 iterations and 3 chains of 20 0000 MCMC iterations, while our models in **Paper III** were specified in JAGS, using an adaptation phase of 15 000 iterations and 3 chains of 30 0000 MCMC iterations. All analyses were performed in Rstudio (Team, 2015) and R version 3.3.1 (Team, 2016). Packages used for modelling are coda (Plummer et al., 2006) and rjags (Plummer, 2016b). For plotting we used ggplot2 (Wickham, 2009), grid (R Core Team, 2016) and cowplot (Wilke, 2016).

Results and Discussion

A summary of the key findings from the work in this study are presented in the following paragraphs. The first part deals with the modified TMH py-GC/MS method and the adapted protocol for *Pinus* species (Objective 1). This is followed by the examination of the in-depth eco-physiological response of UV-B absorbing compounds in *Pinus* spp. pollen and effects of UV-B radiation (Objective 2), under the following headings; (i) Species-level variation in *Pinus* spp., (ii) Results of short-term changes and timing of the UV-B response in *Pinus* spp. and (iii) Short-term plasticity effect and timing of the UV-B response in *Pinus* spp.

Modified TMH py-GC/MS technique

As stated previously, sample reproducibility is a known problem in TMH with py-GC/MS. Preliminary studies indicate that raw *p*CA values are relatively susceptible to machine variance between runs, and may therefore yield low sample reproducibility. Our first objective in ***Paper I*** was to investigate whether this could be improved through introducing an internal standard in order to measure the relative ratios of *p*CA and NAA.

The analytical precision of the ions representative of the *p*CA from the calibration solutions ranges between 4.5-12.9% (mean RSD: 8.3%) for m/z 161 and 4.8- 13.2% (mean RSD: 8.9%) for m/z 192. When these ions are standardized by our internal standard (NAA) which is represented by ions m/z 74, m/z 87 and m/z 312, the RSD is approximately halved (Fig. 6 a, b). The lowest RSD (1.1-4.0%) of the calibration solution with internal standard is achieved using m/z 161 (*p*CA) and m/z 74 (NAA) (Fig. 6 b). There is a strong linear relationship between the known ratios in the calibration solutions and the ratio between the ions m/z 161 and m/z 74 detected in the GC (Adjusted $r^2 = 0.998$, $p < 0.001$). We expect NAA to have a similar reaction efficiency as *p*CA released from the sporopollenin since NAA is a carboxylic acid. As a result, we also expect it to behave in a similar way in the TMAH reaction. This is probably the reason why the analytical precision of the *p*CA (m/z 161 and m/z 192) is approximately doubled when we standardize the peak area by the NAA (m/z 74). As a result, a

calibration solution is run between every second pollen sample to detect and correct for between batch variance, column cut variance and machine variance.

The chromatogram from the mean spectra revealed a small secondary peak at 16.7 minutes while the main *p*CA peak was at 17.7 minutes retention time, see Paper II. In the full scan of the *Pinus* pollen, the small secondary peak was also overlaid with an additional compound (Benzoic acid, 3,4-dimethoxy-); however these two compounds can be separated by extracting the m/z 161 or m/z 192 ion. The retention time of Nonadecanoic acid in the sample containing the internal standard was 24.3 minutes. Although this compound is a chemical homologue to other compounds of the sporopollenin, it was not observed in the *Pinus sylvestris* pollen samples analysed without the addition of this internal standard. This is critical, as the internal standard (NAA) should not be present in the sporopollenin compounds to give an accurate *p*CA ratio. Blokker et al. (2006) identified ferulic acid in *Alnus* spp. pollen which is another UV-B absorbing compound; however, this was not detected within the 200-grain *Pinus sylvestris* pollen. This suggests that analyses should be carefully designed for specific plant genera.

Our final analysis in ***Paper I*** aimed to test whether a ratio approach could be extended to quantify *p*CA in *Pinus sylvestris* pollen grains. Results from this analysis show a strong positive linear relationship (Adjusted $r^2 = 0.958$, $p < 0.001$) between increasing number of grains and the ratio of *p*CA: NAA (Fig. 7 a). The slope of the regression is highly significant, showing the capability of the ratio method to detect changes in *p*CA, and demonstrates the potential for this method to be used as a pollen-based UV-B proxy. The signal-to-noise ratio starts to flatten out after around 250 grains (Fig. 7 b). Although the best signal-to-noise ratio is at 250 grains, 150 grains will still likely be adequate for quantitative analysis in samples with low numbers of pollen grains (e.g. pollen from sediment core samples).

We also conducted a series of other tests, we investigating; (i) the amount of TMAH applied to pollen samples, (ii) different baking times with TMAH (iii) py-GC/MS analyses with different split ratios and iv) using Anthracene as internal standard. None

of these tests gave significant results and all showed minimal effects on the overall yield of the pollen *p*CA abundance.

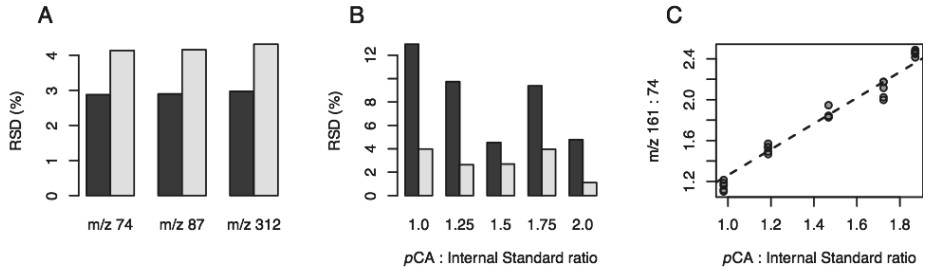

Figure 6. Results from the tests to improve analytical precision in our system set-up. **a)** Mean RSD of the m/z 161 (dark grey bars) and the m/z 192 ions (light grey bars) from the standards, divided by different ion combinations from the NAA peak (m/z 74, 87, 312). **b)** Comparisons of the RSD from the raw m/z 161 peak and the peak when standardised by the m/z 74 peak for the five different standard concentrations. **c)** Comparisons of the estimated pCA: NAA ratio compared with the known ratio in the five standard solutions using the m/z 161: 74 ions.

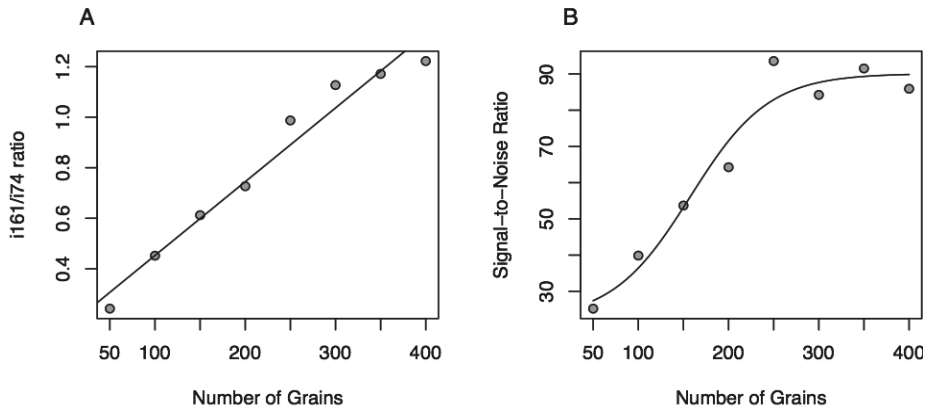

Figure 7. a) Estimated p-CA: NAA ratio (m/z 161 intensity) measured against the number of grains loaded into the sample. **b)** Signal-to-noise ratio of m/z 161 in relation to the number of grains.

Species-level variation in Pinus spp.

In ***Paper II*** we investigated whether *Pinus* species have different *p*CA abundance. Our results show strong species-level variation in the pollen samples from the Geneva Botanic Gardens, which can be partially accounted for by pollen size. *Pinus pinaster* contained up to twice the amount of *p*CA compared with the other species. One obvious explanation for these differences is pollen size. In general, *P. pinaster* pollen grains are approximately two times larger in biovolume than the other species. Indeed, when we correct for this using Beug (1961)'s reported average pollen size, the difference between species is reduced (Fig. 8 and 10 C, D). This effect is most obvious for *P. peuce, P. pinaster* and *P. nigra.* But even when this is corrected for, we still see species-level differences and *Pinus pinaster* still showed higher *p*CA ratios compared with the other species (Fig. 8 and 9 c, d). *P. nigra*, for instance, is aligned with *P. peuce* and *P. pinaster* after pollen size correction, and shows greater differences with *P. sylvestris* and *P. uncinata*. This is likely to be because Beug (1961)'s reported average pollen size is not completely representative for the *Pinus* spp. pollen size in our study. *P. nigra* is downsized when actual pollen size is similar to *P. sylvestris* (Fig. A1 and Table A2). One possibility is that there are better ways to correct for pollen size: for example by measuring corpus and sacci and calculating the pollen size of each species. Alternatively, there could be other genetic differences which result in differences in *p*CA abundance or in UV-B response among species.

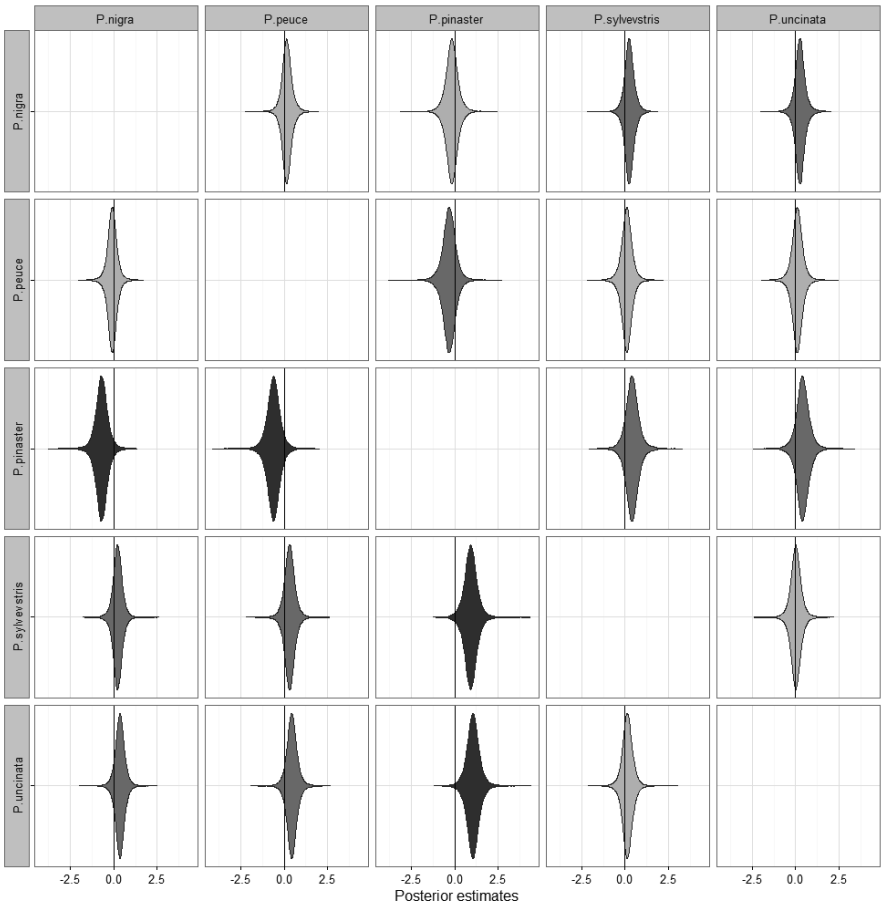

Figure 8. Posterior estimates of difference in pCA between *Pinus nigra*, *P. peuce, P. pinaster*, *P. sylvestris* and *P. uncinata* in Geneva. Bottom left are species-level variation using original pCA ratios and top right are when pollen size corrections have been applied to pCA ratios. Dark grey indicates that the 95% credible intervals do not overlap 0, e.g. the species-level variation is credibly different. Mid grey indicates that the 80% credible intervals do not overlap 0, e.g. the species-level variation is slightly different.

Results of short-term changes and timing of the UV-B response in Pinus spp.

In ***Paper II*** and ***III*** we investigated whether *Pinus* spp. have a plastic response of *p*CA to short-term changes in UV-B radiation, and the timing of the response of *p*CA, respectively. In the experiment investigating responses between years, the UV-B radiation in April-May 2014 was 1034 J m^2 higher compared with that in April-May 2013 (standardised anomaly of UV-B two months prior to dehiscence was 0.13 in 2014 and -1.24 in 2013), while there were small differences in UV-B exposure between the two previous growing seasons (Fig. 5). *Pinus* spp. responded by producing 24% more *p*CA in 2014 under these natural differences (Fig. 9 b, d).

In April-May 2014 the Arboretum and Botanical Garden at Milde received a total UV-B radiation of 2153 J m^2 and 90% shading thus resulted in UV-B radiation of 215 J m^2 during the last month before dehiscence. The shaded pollen produced 21% less *p*-Coumaric acid than the sun-exposed pollen (Fig. 9 a). The individual trees showed differences in how strongly they responded to the shading treatment; three trees barely had a reduction in *p*CA production, whilst seven trees showed a strong response to shading (Fig. 9 c). The 95% credible interval of the differences between the two treatment means and the two-year means did not cross zero, providing strong statistical support that *p*CA abundance was different between both the treatments and the years for all species tested, see Paper II (*Pinus nigra, P. pinaster, P. sylvestris* and *P. uncinata*).

In ***Paper III*** we explore the timing of the response of *p*CA. Our results show that the statistical analyses with the full dataset have decreasing slope coefficients from weakly positive to negative the further back we go through the pollen development period. The DIC values show a slight decrease towards dehiscence date; however, there are minor differences between the predictor variables. The poor model fit of the full data set is mainly because of Benmore and Edinburgh, as they appear to be outliers in all plots (Fig. A2). We therefore decided to analyse the UV-B timing relationship without samples from Benmore and Edinburgh. Both data sets indicate UV-B radiation during the last two weeks before dehiscence as the predictor variable that best explains *p*CA production in *Pinus sylvestris* across Europe (Fig.10 and Fig. A2).

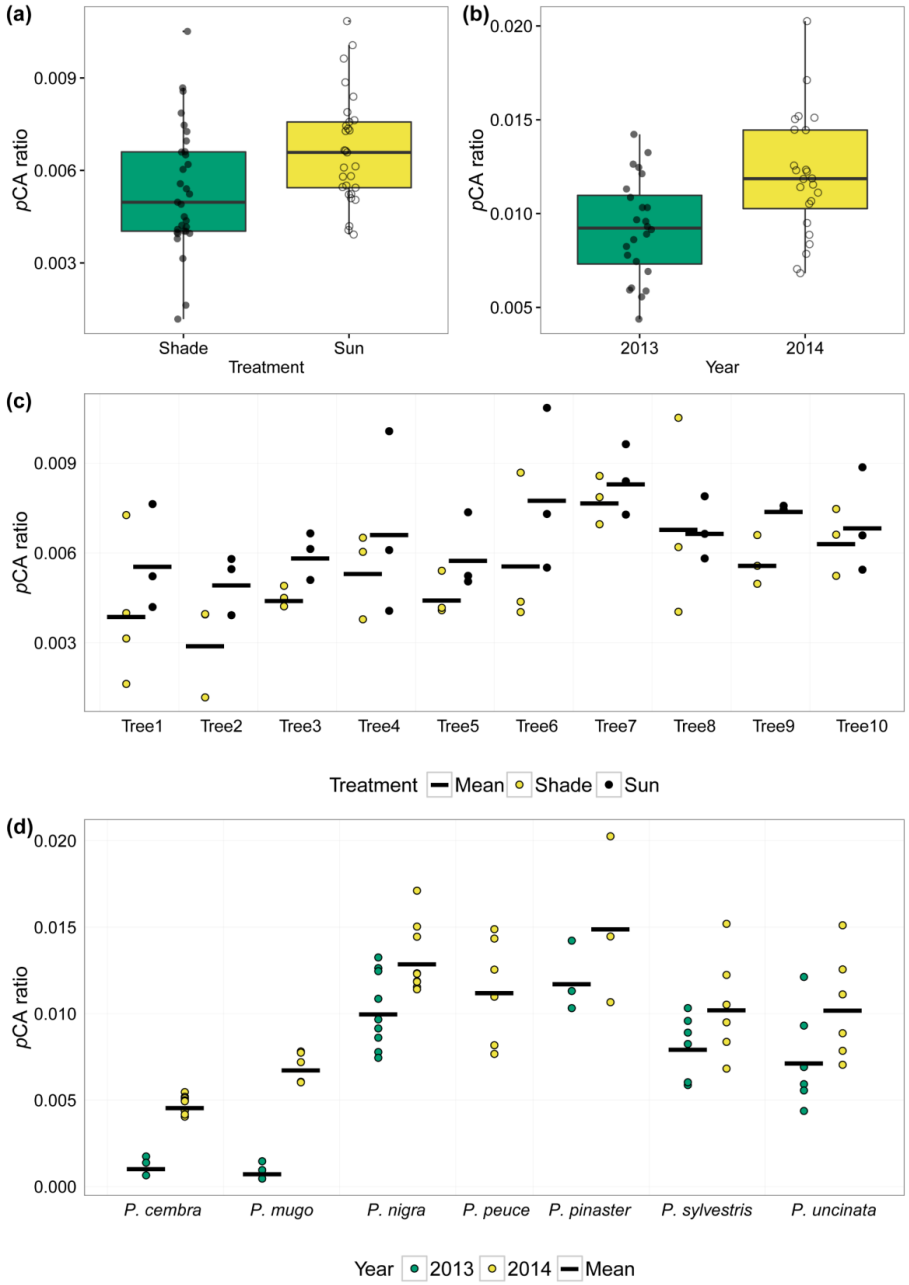

Figure 9. a) Boxplot of shaded (green) and sun-exposed (yellow) *Pinus sylvestris* pollen. The points represent all samples analysed for *p*CA. **b)** Boxplot of *Pinus* spp. pollen from 2013 (green) and 2014 (yellow). The points represent samples of *Pinus nigra, P. pinaster, P. sylvestris* and *P. uncinata* analysed for *p*CA. **c)** Scatterplot of individual trees showing the response of the shaded (green circles) and sun-exposed (yellow circles) *Pinus sylvestris* pollen, black line is the mean for each tree. **d)** Scatterplot of *Pinus* spp. showing the response of *p*CA to different UV-B radiation in Geneva when pollen-grain size is accounted for. *Pinus* spp. pollen in 2013 (green circles) and 2014 (yellow circles), black line is the mean for each species. The boxplots shows 1st and 3rd quartile, horizontal line within is the median and the whiskers show minimum and maximum values, excluding two outliers in **a)**.

In the statistical analyses without Benmore and Edinburgh, the two weeks (14 days) before dehiscence is the UV-B radiation period that best explains *p*CA production in *Pinus sylvestris* pollen (CRI above zero: 99.9, DIC: -8.013, Fig. 10). There is a strong linear relationship with higher UV-B during the two weeks before dehiscence (Fig. 11 b). The second best predictor variable is mean UV-B one week before dehiscence (7 days, CRI above zero: 99.4, DIC: -7.293) (Fig. 11 a) and then three weeks (35 days, CRI above zero: 98.9, DIC: -7.216) before dehiscence (Fig. 10, Fig. A2). When going further back than the last three weeks, the DIC plateaus at c. -7.0. This is the same for pollen bud growing season and mean long-term UV-B radiation (Fig. 10 c).

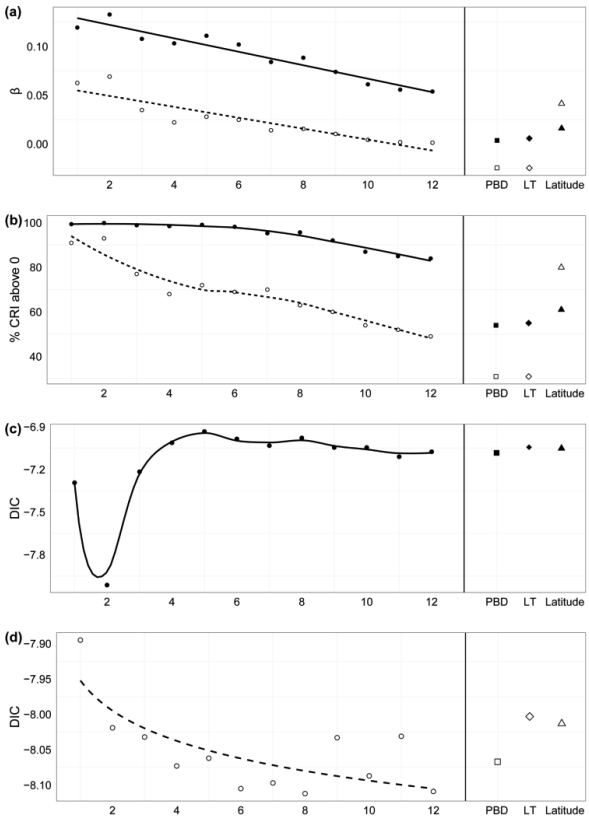

Figure 10. a) Slope values and **b)** % of the slope credible interval (CRI) above zero and **c** and **d)** DIC values for *p*CA across Europe against different UV-B time models. Black lines and symbols is data analysed without Benmore and Edinburgh while dotted line and hollow symbols included these arboreta. Circles represents models of *p*CA fitted against mean UV-B radiation from one week to twelve weeks before to dehiscence in *Pinus sylvestris*, squares represent models of *p*CA fitted against UV-B during July-October 2013 (PBD), diamonds represent models of *p*CA fitted against mean long-term UV-B (LT), and triangles represent models of *p*CA fitted against latitude.

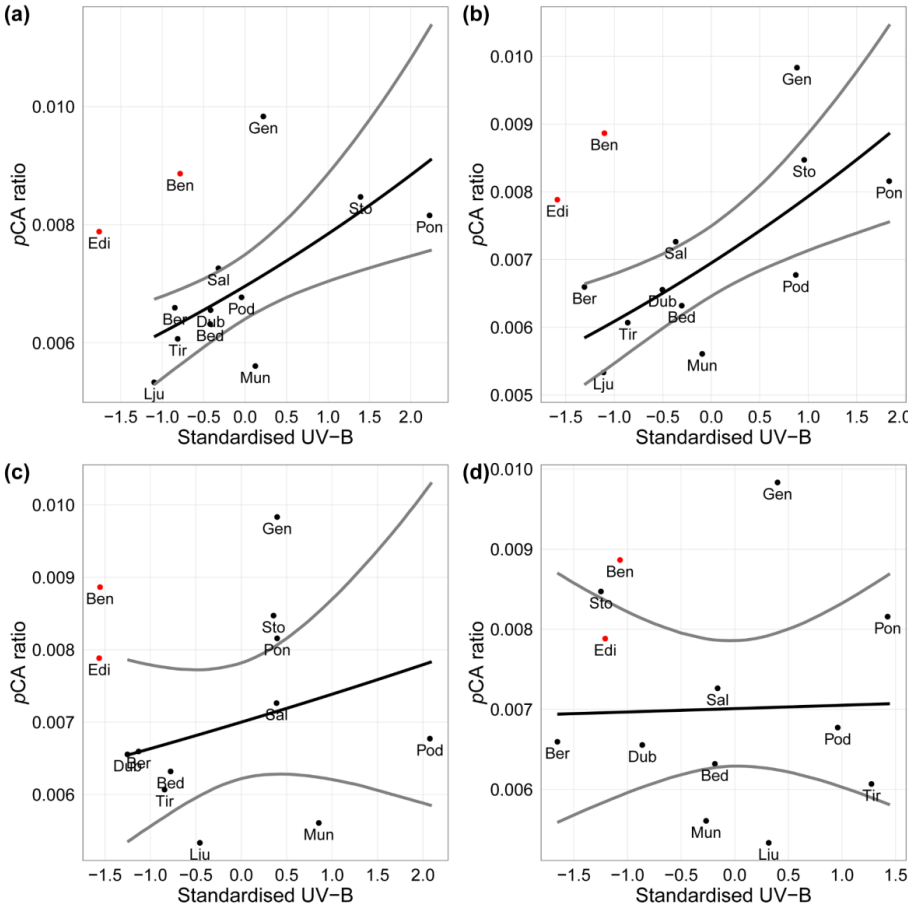

Figure 11. Measured *p*-coumaric acid (*p*CA) ratios in black circles. Red circles are Benmore and Edinburgh. The regression line is calculated from the posterior estimates of the model (black) on predicted *p*CA production in *Pinus sylvestris* (analysed without Benmore and Edinburgh) with a 95% credible interval (grey lines) against **a)** mean UV-B radiation during the one week, **b)** the two weeks and **c)** the twelve weeks immediately before dehiscence across Europe and **d)** mean long-term UV-B.

Short-term plasticity effect and timing of the UV-B response in Pinus spp.

Combined, the results from our studies reveal a plastic response of UV-B absorbing compounds in *Pinus* spp. to short-term UV-B radiation. The work of Lomax *et al.* (2008) showed a positive correlation between phenolic acid concentration in *Lycopodium* spores with growing season UV-B across a 30-year period.

These results support the current understanding of pollen formation within *Pinus* spp. Although the pollen bud starts growing in the previous season, the pollen grains within the bud start developing two to three months before dehiscence. During the last stages in pollen grain development, the peritapetal membrane that contains sporopollenin (e.g. *p*CA) is produced and covers the exine (Dickinson and Bell, 1972, Rowley et al., 2000). The tapetal cells which produce the peritapetal membrane most likely play an important role in production of *p*CA, and this final stage happens less than 11 days before dehiscence (Rowley et al., 2000). We observe that in Geneva there was no difference in surface UV-B between the growing seasons of 2013 and 2014, but there was a large difference in pollen season UV-B radiation, in both one month and two months prior to dehiscence (***Paper II***). A short-term pollen season response is thus the only way to explain the considerable difference in *p*CA between the two years. This is further supported by the shading experiment, where the shade cloth was put in one month before pollen dehiscence and a similar effect was observed (***Paper II***). As the shading cloth treatment was conducted for individual branches within trees, this experiment also indicates that this plastic response to a short-term reduction in UV-B radiation occurs locally within the tree, at the cone bud level. ***Paper III*** strengthens these findings by indicating that UV-B radiation during the last two weeks before dehiscence are the predictor variables that best explains *p*CA abundance in *Pinus sylvestris* across Europe.

Further support for the importance of the peritapetal membrane and the short-term plastic response is given by the very low amount of *p*CA in the *Pinus cembra* and *Pinus mugo* pollen from Geneva in 2013. These pollen bud cones were collected before they were fully mature, which resulted in underdeveloped and transparent pollen. We decided to exclude these species from any subsequent statistical analyses, as we infer that the peritapetal membrane containing *p*CA had not yet been developed or was in an early

stage. This also highlights the importance of sampling fully mature pollen during dehiscence.

Implications for palaeoecological reconstructions

Our findings have implications for the usage of *p*CA as a UV-B proxy in palaeoecological reconstructions. First, our findings indicate that the production of *p*CA is a plastic, short-term response to the environment, which implies that pollen grains from a given tree sampled across multiple years should accurately reflect changes in the local UV-B signal during the dehiscence season. Second, pollen-chemistry measurements taken from sediment cores will represent an integrated seasonal UV-B flux across the range of years represented in a given sediment sample. Depending on sedimentation rate and temporal resolution, a typical sample from the pollen record represents anywhere between 5 and 20 years, and any between-year variation in pollen season UV-B is therefore averaged out, giving us confidence that we can observe long-term trends (e.g., (Willis et al., 2011)). In addition, strong abrupt changes in past UV-B, such as from large volcanic eruptions, are likely to be picked up by the proxy due to their massive impact on climate and the biosphere (Rampino and Self, 1992, de Silva and Zielinski, 1998). Finally, the species-level variation observed in our study implies that in sediment cores sampled in an area with a known occurrence of several species of *Pinus*, UV-B reconstructions may be more difficult. This is especially the case if these species vary greatly in pollen size (for example, in Spain *Pinus nigra, P. pinaster* and *P. sylvestris* have overlapping range areas (Debreczy et al., 2011)). Given these complexities, we expect that applying size corrections to *p*CA ratios could improve the accuracy of the reconstruction of past UV-B radiation, especially if specific size-correction factors for a given site can be established.

Conclusions

We have successfully modified a methodology to ensure more precise quantitative determination of UV-B absorbing compounds in *Pinus* spp. Results indicated that achieving precision using standard pyrolysis systems can be challenging, but that the use of an internal standard within the reaction phase can have major implications for the results. Analysis of the chromatograms revealed major differences in the chemical spectra of *P. sylvestris* pollen and *Alnus* spp. pollen. Large species-level variation is also found, which is only partly explained by pollen size. These results indicate the importance of carefully designing a proxy for specific plant species.

We then used this method to investigate the effect of short-term change in UV-B radiation on production in *p*CA in *Pinus* spp. pollen, the timing of the response, and also species-level variation. Our results demonstrate a short-term plastic response in *p*CA production in *Pinus* spp. pollen due to short-term changes in UV-B radiation in (i) the shading experiment, (ii) the two-year comparison and (iii) across Europe. The tapetal cells which produce the peritapetal membrane most likely play an important role in the production of *p*CA. *p*CA abundance shows strong species-level variation, largely reflecting differences in pollen size between species. Our findings support the usage of *p*CA as a UV-B proxy in palaeoecological reconstructions. However, given the strong indication of short-term plastic response to changes in UV-B radiation, we suggest that the proxy reflects a seasonal response. Nevertheless, we expect that the signal integrated across years found in a pollen record will be able to accurately detect longer term changes in past UV-B flux. using *Pinus* spp. as proxy, and we highlight the importance of accounting for species-level variation in reconstructions.

Challenges and Future work

Our results indicate that there is within-tree variation. In both the shading experiment and the two-year comparison study we see large ranges in *p*CA within single trees and one botanical garden, even within controls. The results of the shading experiment indicate that some of this variation could be explained by local responses within the tree, at the scale of individual branches or flowers. A more strongly correlated signal may have been obtained in ***Paper III*** if the number of *Pinus sylvestris* were increased (our data contains one tree of *Pinus sylvestris* in 11 of the 13 arboreta) since some arboreta show high within-tree variation. Alternatively, the relationship could have been strengthened by including a greater number of *Pinus* species per arboretum.

As a result of local within-tree variation responses, we might see successional effects in the palaeoecological record. As the forest grows denser and taller less light is available, which may affect the signal. However, since *Pinus* spp. are shade-intolerant, such impacts should be relatively minor. Furthermore, pollen from a sediment core is also an integrated signal across many trees and has a relatively large spatial extent since it is a wind-pollinated species e.g. *Pinus* species is known to disperse pollen over long distances (Birks et al., 2016)

Since *p*CA in pollen is only representative of surface UV-B radiation during spring time, we would need to look elsewhere for an annual proxy. One possibility would be to explore the production of *p*CA in stomata of needles of *Pinus* spp. Since needle production is related to the growing season temperature in the year before production (Junttila and Heide, 1981, Huusko and Hicks, 2009), it is possible that needles respond to UV-B influx during the previous growing season.

Future research proposals

The results from this thesis are novel and contribute important implications for the THM py-GC/MC method and the use of a *Pinus* spp. pollen-based UV-B proxy. It opens the door for future investigations into the drivers of change of pollen-chemistry. There are a number of research questions that remain to be answered.

1. Since our results show that *Pinus* spp. pollen represents seasonal UV-B radiation, an interesting future research question is whether *p*CA abundance in *Pinus* spp. needles can represent an annual or possibly an integrated UV-B proxy of several years. As *Pinus* spp. needles have a life span of c. 2-3 or more years and are preserved in the sedimental record. They may be able to provide a more robust proxy of changes in past UV-B flux.
2. Our results demonstrate a short-term plastic response in the artificial shading experiment with 90% shading. An interesting future research question is whether a linear dose-response relationship can be established. A field experiment can be initiated in a *Pinus* orchard where the trees have the same genetic origin, and a full range of shading variables; 30%, 50%, 70%, 90% and full sun exposure can be tested. In addition, UV-B loggers could be used to record the amount of UV-B radiation in each treatment. I hypothesize a decrease in between tree-variation of *p*CA abundance because of same genetic difference.
3. Our results indicate that the timing of the response of pCA abundance is determined by the UV-B during the last two weeks before dehiscence. An interesting future research question is whether an experiment yield similar results of timing of the response of pCA abundance as the results from the study across Europe. This can be done by initiating an experiment where trees from multiple *Pinus* spp. are covered with a 90% shade cloth, starting two months prior to dehiscence, and cover a new branch every week until dehiscence. Bedgebury National Pinetum would be an excellent study site since it has several trees per *Pinus* species.
4. Since the *Pinus* spp. pollen proxy will represent an integrated seasonal UV-B flux across the range of years represented in a given sample, an interesting future research question is whether the 1600 A.D. Huaynaputina in Peru or the super-eruption of Toba in Sumatra 73 500 years ago can be detected in a pollen chemistry UV-B proxy.

5. Our Bayesian framework is part of the next generation statistical analyses and our work founds the platform for future palaeoecological inference. Further development of Bayesian inference in palaeoecological reconstructions could potentially incorporate uncertainty models of pollen dispersal and in-depth age models.

References

ABAD VIÑAS, R., CAUDULLO, G., OLIVEIRA, S. & DE RIGO, D. 2016. *Pinus pinaster* in Europe: distribution, habitat, usage and threats. *In:* SAN-MIGUEL-AYANZ, J., DE RIGO, D., CAUDULLO, G., HOUSTON DURRANT, T. & MAURI, A. (eds.) *European Atlas of Forest Tree Species.* Publication Office of the European Union: Luxembourg.

AROLA, A., KAZADZIS, S., LINDFORS, A., KROTKOV, N., KUJANPAA, J., TAMMINEN, J., BAIS, A., DI SARRA, A., VILLAPLANA, J. M., BROGNIEZ, C., SIANI, A. M., JANOUCH, M., WEIHS, P., WEBB, A., KOSKELA, T., KOUREMETI, N., MELONI, D., BUCHARD, V., AURIOL, F., IALONGO, I., STANECK, M., SIMIC, S., SMEDLEY, A. & KINNE, S. 2009. A new approach to correct for absorbing aerosols in OMI UV. *Geophysical Research Letters,* 36.

BALLARE, C. L., CALDWELL, M. M., FLINT, S. D., ROBINSON, A. & BORNMAN, J. F. 2011. Effects of solar ultraviolet radiation on terrestrial ecosystems. Patterns, mechanisms, and interactions with climate change. *Photochemical & Photobiological Sciences,* 10**,** 226-241.

BALLARE, C. L., ROUSSEAUX, M. C., SEARLES, P. S., ZALLER, J. G., GIORDANO, C. V., ROBSON, T. M., CALDWELL, M. M., SALA, O. E. & SCOPEL, A. L. 2001. Impacts of solar ultraviolet-B radiation on terrestrial ecosystems of Tierra del Fuego (southern Argentina) - An overview of recent progress. *Journal of Photochemistry and Photobiology B-Biology,* 62**,** 67-77.

BALLIAN, D., RAVAZZI, C., DE RIGO, D. & CAUDULLO, G. 2016. *Pinus mugo* in Europe: distribution, habitat, usage and threats. *In:* SAN-MIGUEL-AYANZ, J., DE RIGO, D., CAUDULLO, G., HOUSTON DURRANT, T. & MAURI, A. (eds.) *European Atlas of Forest Tree Species.* Publication Office of the European Union: Luxembourg.

BEERLING, D. J., HARFOOT, M., LOMAX, B. & PYLE, J. A. 2007. The stability of the stratospheric ozone layer during the end-Permian eruption of the Siberian Traps. *Philosophical Transactions of the Royal Society a-Mathematical Physical and Engineering Sciences,* 365**,** 1843-1866.

BEUG, H.-J. 1961. *Leitfaden der Pollenbestimmung für Mitteleuropa and angrenzende Gebiete : Lieferung 1,* Stuttgart, Gustav Fisher.

BIRKS, H. J. B., FELDE, V. A., BJUNE, A. E., GRYTNES, J.-A., SEPPÄ, H. & GIESECKE, T. 2016. Does pollen-assemblage richness reflect floristic richness? A review of recent developments and future challenges. *Review of Palaeobotany and Palynology,* 228**,** 1-25.

BJORN, L. O. & MCKENZIE, R. L. 2007. Attempts to probe the ozone layer and the ultraviolet-B levels of the past. *Ambio,* 36**,** 366-371.

BLOKKER, P., BOELEN, P., BROEKMAN, R. & ROZEMA, J. 2006. The occurrence of p-coumaric acid and ferulic acid in fossil plant materials and their use as UV-proxy. *Plant Ecology,* 182**,** 197-207.

BLOKKER, P., YELOFF, D., BOELEN, P., BROEKMAN, R. A. & ROZEMA, J. 2005. Development of a proxy for past surface UV-B irradiation: A thermally assisted hydrolysis and methylation py-GC/MS method for the analysis of pollen and spores. *Analytical Chemistry,* 77**,** 6026-6031.

BORNMAN, J. F., BARNES, P. W., ROBINSON, S. A., BALLARE, C. L., FLINT, S. D. & CALDWELL, M. M. 2015. Solar ultraviolet radiation and ozone depletion-driven climate change: effects on terrestrial ecosystems. *Photochemical & Photobiological Sciences,* 14**,** 88-107.

CALDWELL, M. M., BALLARE, C. L., BORNMAN, J. F., FLINT, S. D., BJORN, L. O., TERAMURA, A. H., KULANDAIVELU, G. & TEVINI, M. 2003. Terrestrial ecosystems increased solar ultraviolet radiation and interactions with other climatic change factors. *Photochemical & Photobiological Sciences,* 2**,** 29-38.

CALDWELL, M. M., BORNMAN, J. F., BALLARE, C. L., FLINT, S. D. & KULANDAIVELU, G. 2007. Terrestrial ecosystems, increased solar ultraviolet radiation, and interactions with bother climate change factors. *Photochemical & Photobiological Sciences,* 6**,** 252-266.

CLARKE, A. & GASTON, K. J. 2006. Climate, energy and diversity. *Proceedings of the Royal Society B-Biological Sciences,* 273**,** 2257-2266.

DAVIES, T. J., SAVOLAINEN, V., CHASE, M. W., MOAT, J. & BARRACLOUGH, T. G. 2004. Environmental energy and evolutionary rates in flowering plants. *Proceedings of the Royal Society B-Biological Sciences,* 271**,** 2195-2200.

DAWSON, A., PACIOREK, C. J., MCLACHLAN, J. S., GORING, S., WILLIAMS, J. W. & JACKSON, S. T. 2016. Quantifying pollen-vegetation relationships to reconstruct ancient forests using 19th-century forest composition and pollen data. *Quaternary Science Reviews,* 137**,** 156-175.

DE SILVA, S. L. & ZIELINSKI, G. A. 1998. Global influence of the AD 1600 eruption of Huaynaputina, Peru. *Nature,* 393**,** 455-458.

DEBRECZY, Z., RÁCZ, I. & MUSIAL, K. 2011. *Conifers around the world : conifers of the temperate zones and adjacent regions : Vol. 1,* Budapest, Dendro Press.

DEMKURA, P. V., ABDALA, G., BALDWIN, I. T. & BALLARE, C. L. 2010. Jasmonate-Dependent and -Independent Pathways Mediate Specific Effects of Solar Ultraviolet B Radiation on Leaf Phenolics and Antiherbivore Defense. *Plant Physiology,* 152**,** 1084-1095.

DI-GIOVANNI, F., KEVAN, P. G. & CARON, G. É. 1996. Estimating the timing of maximum pollen release from jack pine (Pinus banksiana Lamb.) in northern Ontario. *The Forestry Chronicle,* 72**,** 166-169.

DICKINSON, H. G. 1970. The fine structure of a peritapetal membrane investing the microsporangium of Pinus banksiana. *New Phytologist,* 69**,** 1065-&.

DICKINSON, H. G. & BELL, P. R. 1972. The role of the tapetum in the formation of sporopollenin-containing structures during microsporogenesis in Pinus banksiana. *Planta,* 107**,** 205-215.

DICKINSON, H. G. & BELL, P. R. 1976. The changes in the tapetum of Pinus banksiana. Accompanying formation and maturation of the pollen. *Annals of Botany,* 40**,** 1101-1109.

ENESCU, C. M., DE RIGO, D., CAUDULLO, G., MAURI, A. & HOUSTON DURRANT, T. 2016. *Pinus nigra* in Europe: distribution, habitat, usage and threats. *In:* SAN-MIGUEL-AYANZ, J., DE RIGO, D., CAUDULLO, G., HOUSTON DURRANT, T. & MAURI, A. (eds.) *European Atlas of Forest Tree Species.* Publication Office of the European Union: Luxembourg.

FLENLEY, J. R. 2007. Ultraviolet insolation and the tropical rainforest; altitudinal variations, Quaternary and recent change, extinctions, and biodiversity. *In:* BUSH, M. B. & FLENLEY, J. R. (eds.) *Tropical Rainforest Responses to Climatic Change.* Berlin: Springer.

FOSTER, C. B. & AFONIN, S. A. 2005. Abnormal pollen grains: an outcome of deteriorating atmospheric conditions around the Permian - Triassic boundary. *Journal of the Geological Society,* 162**,** 653-659.

FRASER, W. T., SCOTT, A. C., FORBES, A. E. S., GLASSPOOL, I. J., PLOTNICK, R. E., KENIG, F. & LOMAX, B. H. 2012. Evolutionary stasis of sporopollenin biochemistry revealed by unaltered Pennsylvanian spores. *New Phytologist,* 196**,** 397-401.

FRASER, W. T., SEPHTON, M. A., WATSON, J. S., SELF, S., LOMAX, B. H., JAMES, D. I., WELLMAN, C. H., CALLAGHAN, T. V. & BEERLING, D. J. 2011. UV-B absorbing pigments in spores: biochemical responses to shade in a high-latitude birch forest and implications for sporopollenin-based proxies of past environmental change. *Polar Research,* 30**,** 6.

GELMAN, A. & HILL, J. 2007. *Data analysis using regression and multilevel/hierarchical models,* Cambridge, Cambridge University Press.

GIBB, S. & STRIMMER, K. 2012. MALDIquant: a versatile R package for the analysis of mass spectrometry data. Bioinformatics 2270–2271.

HAYLOCK, M. R., HOFSTRA, N., KLEIN TANK, A. M. G., KLOK, E. J., JONES, P. D. & NEW, M. 2008. A European daily high-resolution gridded data set of surface temperature and precipitation for 1950–2006. *Journal of Geophysical Research: Atmospheres,* 113**,** D20119.

HERMAN, J. R. 2010. Global increase in UV irradiance during the past 30 years (1979-2008) estimated from satellite data. *Journal of Geophysical Research-Atmospheres,* 115.

HOLDEN, P. B., BIRKS, H. J. B., BROOKS, S. J., BUSH, M. B., HWANG, G. M., MATTHEWS-BIRD, F., VALENCIA, B. G. & VAN WOESIK, R. 2016. BUMPER v1.0: A Bayesian User-friendly Model for Palaeo-Environmental Reconstruction. *Geosci. Model Dev. Discuss.,* 2016**,** 1-21.

HOUSTON DURRANT, T., DE RIGO, D. & CAUDULLO, G. 2016. *Pinus sylvestris* in Europe: distribution, habitat, usage and threats. *In:* SAN-MIGUEL-AYANZ, J., DE RIGO, D., CAUDULLO, G., HOUSTON DURRANT, T. & MAURI, A. (eds.) *European Atlas of Forest Tree Species.* Publication Office of the European Union: Luxembourg.

HUUSKO, A. & HICKS, S. 2009. Conifer pollen abundance provides a proxy for summer temperature: evidence from the latitudinal forest limit in Finland. *Journal of Quaternary Science,* 24**,** 522-528.

JACKSON, S. T. 2012. Representation of flora and vegetation in Quaternary fossil assemblages: known and unknown knowns and unknowns. *Quaternary Science Reviews,* 49**,** 1-15.

JARDINE, P. E., FRASER, W. T., LOMAX, B. H. & GOSLING, W. D. 2015. The impact of oxidation on spore and pollen chemistry. *Journal of Micropalaeontology,* 34**,** 139-149.

JUNGFERMANN, C., AHLERS, F., GROTE, M., GUBATZ, S., STEUERNAGEL, S., THOM, I., WETZELS, G. & WIERMANN, R. 1997. Solution of sporopollenin and reaggregation of a sporopollenin-like material: A new approach in the sporopollenin research. *Journal of Plant Physiology,* 151**,** 513-519.

JUNTTILA, O. & HEIDE, O. M. 1981. Shoot and needle growth in pinus-sylvestris as related to temperature in northern fennoscandia. *Forest Science,* 27**,** 423-430.

KALAKOSKI, N. 2012. *OMI Level 3 OMUVBd read me file,* Finland, Finnish Meteorological Institute.

LEE, D. W. & LOWRY, J. B. 1980. Solar Ultraviolet on Tropical Mountains - Can It Affect Plant Speciation. *American Naturalist,* 115**,** 880-883.

LI, F. R., PENG, S. L., CHEN, B. M. & HOU, Y. P. 2010. A meta-analysis of the responses of woody and herbaceous plants to elevated ultraviolet-B radiation. *Acta Oecologica-International Journal of Ecology,* 36**,** 1-9.

LIU, J. Q., WANG, Y. J., WANG, A. L., HIDEAKI, O. & ABBOTT, R. J. 2006. Radiation and diversification within the Ligularia-Cremanthodium-Parasenecio complex (Asteraceae) triggered by uplift of the Qinghai-Tibetan Plateau. *Molecular Phylogenetics and Evolution,* 38**,** 31-49.

LLORENS, L., BADENES-PEREZ, F. R., JULKUNEN-TIITTO, R., ZIDORN, C., FERERES, A. & JANSEN, M. A. K. 2015. The role of UV-B radiation in plant sexual reproduction. *Perspectives in Plant Ecology Evolution and Systematics,* 17**,** 243-254.

LOMAX, B. H. & FRASER, W. T. 2015. Palaeoproxies: botanical monitors and recorders of atmospheric change. *Palaeontology,* 58**,** 759-768.

LOMAX, B. H., FRASER, W. T., SEPHTON, M. A., CALLAGHAN, T. V., SELF, S., HARFOOT, M., PYLE, J. A., WELLMAN, C. H. & BEERLING, D. J. 2008. Plant spore walls as a record of long-term changes in ultraviolet-B radiation. *Nature Geoscience,* 1**,** 592-596.

NEWSHAM, K. K. & ROBINSON, S. A. 2009. Responses of plants in polar regions to UVB exposure: a meta-analysis. *Global Change Biology,* 15**,** 2574-2589.

OWENS, J. N. 2006. The reproductive biology of lodgepole pine. Forest Genetics Council of British Columbia.

OWENS, J. N. & MOLDER, M. 1977. DEVELOPMENT OF LONG-SHOOT TERMINAL BUDS OF WESTERN WHITE-PINE (PINUS-MONTICOLA). *Canadian Journal of Botany-Revue Canadienne De Botanique,* 55**,** 1308-1321.

PINHEIRO, J., BATES, D., DEBROY, S. & SARKAR, D. 2013. nlme: Linear and Nonlinear Mixed Effects Models. [WWW Document]. URL http://CRAN.R-project.org/package=nlme/.

PLUMMER, M. 2016a. JAGS: A program for analysis of Bayesian graphical models using Gibbs sampling. 4.1.0 ed.

PLUMMER, M. 2016b. rjags: Bayesian Graphical Models using MCMC. R package version 4-6. https://CRAN.R-project.org/package=rjags.

PLUMMER, M., BEST, N., COWLES, K. & VINES, K. 2006. CODA: Convergence Diagnosis and Output Analysis for MCMC, R News, vol 6, 7-11.

RAMPINO, M. R. & SELF, S. 1992. Volcanic winter and accelerated glaciation following the Toba super-eruption. *Nature,* 359**,** 50-52.

ROWLEY, J. R., SKVARLA, J. J. & WALLES, B. 2000. Microsporogenesis in Pinus sylvestris L. VIII. Tapetal and late pollen grain development. *Plant Systematics and Evolution,* 225**,** 201-224.

ROZEMA, J., BLOKKER, P., FUERTES, M. A. M. & BROEKMAN, R. 2009. UV-B absorbing compounds in present-day and fossil pollen, spores, cuticles, seed coats and wood: evaluation of a proxy for solar UV radiation. *Photochemical & Photobiological Sciences,* 8**,** 1233-1243.

ROZEMA, J., BROEKMAN, R. A., BLOKKER, P., MEIJKAMP, B. B., DE BAKKER, N., VAN DE STAAIJ, J., VAN BEEM, A., ARIESE, F. & KARS, S. M. 2001a. UV-B absorbance and UV-B absorbing compounds

(para-coumaric acid) in pollen and sporopollenin: the perspective to track historic UV-B levels. *Journal of Photochemistry and Photobiology B-Biology,* 62**,** 108-117.

ROZEMA, J., NOORDIJK, A. J., BROEKMAN, R. A., VAN BEEM, A., MEIJKAMP, B. M., DE BAKKER, N. V. J., VAN DE STAAIJ, J. W. M., STROETENGA, M., BOHNCKE, S. J. P., KONERT, M., KARS, S., PEAT, H., SMITH, R. I. L. & CONVEY, P. 2001b. (Poly)phenolic compounds in pollen and spores of Antarctic plants as indicators of solar UV-B - A new proxy for the reconstruction of past solar UV-B? *Plant Ecology,* 154**,** 9-+.

ROZEMA, J., VAN GEEL, B., BJORN, L. O., LEAN, J. & MADRONICH, S. 2002. Paleoclimate: Toward solving the UV puzzle. *Science,* 296**,** 1621-1622.

ROZEMA, J., VANDESTAAIJ, J., BJORN, L. O. & CALDWELL, M. 1997. UV-B as an environmental factor in plant life: Stress and regulation. *Trends in Ecology & Evolution,* 12**,** 22-28.

RYAN, C. G., CLAYTON, E., GRIFFIN, W. L., SIE, S. H. & COUSENS, D. R. 1988. Snip, a statistics-sensitive background treatment for the quantitative-analysis of pixe spectra in geoscience applications. *Nuclear Instruments & Methods in Physics Research Section B-Beam Interactions with Materials and Atoms,* 34**,** 396-402.

SALONEN, J. S., ILVONEN, L., SEPPA, H., HOLMSTROM, L., TELFORD, R. J., GAIDAMAVICIUS, A., STANCIKAITE, M. & SUBETTO, D. 2012. Comparing different calibration methods (WA/WA-PLS regression and Bayesian modelling) and different-sized calibration sets in pollen-based quantitative climate reconstruction. *Holocene,* 22**,** 413-424.

SEARLES, P. S., FLINT, S. D. & CALDWELL, M. M. 2001. A meta analysis of plant field studies simulating stratospheric ozone depletion. *Oecologia,* 127**,** 1-10.

SHAFFER, J. A. & CERVENY, R. S. 2004. Long-term (250,000 BP to 50,000 AP) variations in ultraviolet and visible radiation (0.175-0.690 mu m). *Global and Planetary Change,* 41**,** 111-120.

STUART, B. H. 2004. *Infrared Spectroscopy : Fundamentals and Applications,* Chichester, Wiley.

TANSKANEN, A., LINDFORS, A., MAATTA, A., KROTKOV, N., HERMAN, J., KAUROLA, J., KOSKELA, T., LAKKALA, K., FIOLETOV, V., BERNHARD, G., MCKENZIE, R., KONDO, Y., O'NEILL, M., SLAPER, H., DEN OUTER, P., BAIS, A. F. & TAMMINEN, J. 2007. Validation of daily erythemal doses from Ozone Monitoring Instrument with ground-based UV measurement data. *Journal of Geophysical Research-Atmospheres,* 112.

TEAM, R. 2015. RStudio: Integrated Development for R. RStudio, Inc., Boston, MA URL http://www.rstudio.com/. Boston, MA: RStudio, Inc.

TEAM, R. C. 2016. R: A language and environment for statistical computing. R Foundation for Statistical Computing, Vienna, Austria. URL https://www.R-project.org/.

TREUTTER, D. 2006. Significance of flavonoids in plant resistance: a review. *Environmental Chemistry Letters,* 4**,** 147-157.

TUTEJA, N., SINGH, M. B., MISRA, M. K., BHALLA, P. L. & TUTEJA, R. 2001. Molecular mechanisms of DNA damage and repair: Progress in plants. *Critical Reviews in Biochemistry and Molecular Biology,* 36**,** 337-397.

VISSCHER, H., LOOY, C. V., COLLINSON, M. E., BRINKHUIS, H., CITTERT, J., KURSCHNER, W. M. & SEPHTON, M. A. 2004. Environmental mutagenesis during the end-Permian ecological crisis. *Proceedings of the National Academy of Sciences of the United States of America,* 101**,** 12952-12956.

WAMPLER, T. P. 2006. *Applied Pyrolysis Handbook,* Boca Raton, Taylor and Francis Group.

WANG, Y. J., PAN, J. T., LIU, S. V. & LIU, J. Q. 2005. A new species of Saussurea (Asteraceae) from Tibet and its systematic position based on ITS sequence analysis. *Botanical Journal of the Linnean Society,* 147**,** 349-356.

WEHLING, K., NIESTER, C., BOON, J. J., WILLEMSE, M. T. M. & WIERMANN, R. 1989. p-Coumaric acid - a monomer in the sporopollenin skeleton. *Planta,* 179**,** 376-380.

WICKHAM, H. 2009. *ggplot2: Elegant Graphics for Data Analysis*, Springer-Verlag New York.

WILKE, C. O. 2016. cowplot: Streamlined Plot Theme and Plot Annotations for 'ggplot2'. R package version 0.6.2. https://CRAN.R-project.org/package=cowplot.

WILLIS, K. J., BENNETT, K. D. & BIRKS, H. J. B. 2009. Variability in thermal and UV-B energy fluxes through time and their influence on plant diversity and speciation. *Journal of Biogeography,* 36**,** 1630-1644.

WILLIS, K. J., FEURDEAN, A., BIRKS, H. J. B., BJUNE, A. E., BREMAN, E., BROEKMAN, R., GRYTNES, J. A., NEW, M., SINGARAYER, J. S. & ROZEMA, J. 2011. Quantification of UV-B flux through time using UV-B-absorbing compounds contained in fossil Pinus sporopollenin. *New Phytologist,* 192**,** 553-560.

ZAVALA, J. A. & RAVETTA, D. A. 2002. The effect of solar UV-B radiation on terpenes and biomass production in Grindelia chiloensis (Asteraceae), a woody perennial of Patagonia, Argentina. *Plant Ecology,* 161**,** 185-191.

Papers and Appendix

I

Paper I

An adapted protocol for reconstructions of surface UV-B radiation using thermally assisted hydrolysis and methylation of *Pinus sylvestris* pollen

Alistair W. R. Seddon, Mari Jokerud, Tanja Barth, H. John B. Birks, Vigdis Vandvik and Kathy J. Willis

Submitted to *Review of Palaeobotany & Palynology*.

For supporting information, see Appendix, A3.

An adapted protocol for reconstructions of surface UV-B radiation using thermally assisted hydrolysis and methylation of Pinus sylvestris pollen

Alistair W. R. Seddon[a,b,*], Mari Jokerud[a], Tanja Barth[c], H. John B. Birks[a,d], Vigdis Vandvik and Kathy J. Willis[e,f,a]

[a]Department of Biology, University of Bergen, Bergen, Norway

[b]Bjerknes Centre for Climate Research, University of Bergen, Norway

[c]Department of Chemistry, University of Bergen, Bergen, Norway

[d]Environmental Research Centre, University College London, UK

[e]Royal Botanic Gardens, Kew, Richmond, Surrey UK

[f]Biodiversity Institute, Oxford Martin School, Department of Zoology University of Oxford, Oxford, UK

**Corresponding author:* alistair.seddon@uib.no

Abstract

UV-B absorbing compounds, such as para-Coumaric acid, are a major constituent of the sporopollenin-based exines of pollen grains. Recent research indicates that these compounds are found in higher concentrations in the pollen of plants exposed to higher levels of UV-B radiation, and studies have proposed that variations of para-Coumaric acid within fossil pollen could act as a proxy for changes in the amount of UV-B reaching the Earth's surface. However, the low analytical precision of currently established methods means quantification of UV-B absorbing compounds within sporopollenin remains a major challenge. Here, we present a new approach which incorporates adding a known quantity of an internal standard (Nonadecanoic acid) to samples prior to analysis using pyrolysis-Gas Chromatography Mass Spectrometry on Pinus sylvestris L. pollen. Nonadecanoic acid is a chemical homologue to other sporopollenin based derivatives of py-GC/MS, and we therefore expect it to have similar reaction efficiencies to other components of the pollen exines. Results from tests on

chemical solutions indicate that the adding of this internal standard leads to an approximate doubling of analytical precision and more robust determination of the abundance of para-Coumaric acid. We also demonstrate that the method is able to detect linear increases in the total amount of para-Coumaric acid in samples containing different numbers of pollen grains. The findings from this study open the door for future comprehensive analytical investigations into the drivers of change of pollen-chemistry signatures in Pinus pollen in the development of a UV-B proxy.

Keywords: fossil pollen; para-Coumaric acid; pyrolysis-Gas Chromatography Mass Spectrometry; sporopollenin; UV-B

Abbreviations:
NAA: Nonadeconoic acid
pCA: para-Coumaric acid
THM: Thermally assisted hydrolysis and methylation
py-GC/MS: Pyrolysis gas chromatography mass spectrometry
UV-B - Ultraviolet radiation (280–315 nm)

1. Introduction

Ultraviolet radiation (UV-B) is known to have major effects on human health, terrestrial ecosystems and biogeochemical cycles (Gao et al., 2010). UV-B is also thought to have experienced large changes throughout Earth's history in response to orbital variations, super-volcanic events and changes in cloud cover (Beerling et al., 2007). As a result, changes in UV-B flux are likely to have had profound influences on climate, biodiversity and terrestrial ecosystem functioning (Foster and Afonin, 2005; Looy et al., 2001; Willis et al., 2009), but reconstructing variations in surface UV-B irradiance over centuries or millennia remains a major challenge. To address the ecological and evolutionary impacts of variability in exposure to surface UV-B radiation in the geological past, work is currently underway to develop a pollen-based UV-B proxy (Blokker et al., 2006, 2005; Lomax and Fraser, 2015; Lomax et al., 2012, 2008; Rozema et al., 2001; Watson et al., 2007; Willis et al., 2011).

Pollen grains are composed of the complex biomolecule sporopollenin (de Leeuw et al., 2006). Although its exact composition remains poorly understood, sporopollenin has been shown to contain UV-B absorbing compounds such as para-Coumaric acid (3-(4-hydroxyphenyl)-2-propenoic acid) (pCA hereafter) and Ferulic acid ((E)-3-(4-hydroxy-3-methoxyphenyl)-2-propenoic acid). Recent research indicates that these compounds are found in higher concentrations in the pollen of plants exposed to higher levels of UV-B (Blokker et al., 2006; Lomax et al., 2008; Rozema et al., 2001; Willis et al., 2011). Because sporopollenin is resistant to degradation when buried in anoxic environments such as lakes and bogs, UV-B absorbing compounds such as pCA and Ferulic acid in pollen grains are thought to be a useful proxy to provide reconstructions of UV-B irradiance on timescales far beyond the instrumental (i.e. the past 40 years) record (Blokker et al., 2006; Lomax et al., 2012, 2008; Rozema et al., 2001; Willis et al., 2011).

Successful application of a pollen-based UV-B proxy involves extracting pollen grains manually from a sediment sample before analysis. Two analytical approaches have then been used to identify chemical variability within the sporopollenin. Fourier transform infrared spectroscopy (FTIR) is relatively quick and can be applied to a small number of grains (Fraser et al., 2012; Jardine et al., 2015; Lomax et al., 2008), but FTIR has the disadvantage of only providing relative abundances after standardisation to the relatively more stable OH groups found within the infrared spectra.

Alternatively, thermally assisted methylation (THM) reaction with pyrolysis-Gas Chromatography Mass Spectrometry (py-GC/MS) (Blokker et al., 2005; Challinor, 2001) uses a strong base reagent (tetraammonium hydroxide, TMAH) to depolymerise the constituents within the sporopollenin and subsequently convert them to methyl esters. These derivatives are chemically stable and thus more readily quantified with py-GC/MS. Although more time consuming, THM py-GC/MS methods have the advantage of being able to provide more highly resolved characterisation of the different phenolic compounds. This may be important because different components of the sporopollenin may respond to the same UV-B radiation dose in different ways (Blokker et al., 2005), implying that py-GC/MS methods may be better suited to track detailed biochemical changes compared to FTIR (Watson et al., 2007). Note, however, that absolute

quantification would never be possible because of the uncertainty arising from the differences in intermolecular linkages that may result in the pyrolysis products (Blokker et al., 2006).

Blokker et al. (2005) first developed a set of protocols to measure changes in the concentrations of UV-B absorbing compounds in Alnus pollen. They investigated whether pCA and Ferulic acid, both present in the pollen exine and known to exhibit strong UV-B absorbing capabilities (Rozema et al., 2001), could be characterised using THM py-GC/MS. They then used this method to investigate UV-B effects on Vicia faba pollen under high and low UV-B conditions in a greenhouse. The method was also applied to (i) test the relationship between sporopollenin-based pCA and UV-B in Pinus spp. across a latitudinal gradient in Europe, and (ii) to reconstruct surface UV-B flux over the last 11,000 years using Pinus spp. pollen grains extracted from a lake-sediment core from western Norway (Willis et al., 2011).

Despite these developments, THM- py-GC/MS analysis of sporopollenin presents a major analytical challenge. Measurements of py-GC/MS derivatives can be characterised by high variance and, as a consequence, low analytical precision. For example, a recent study found that the relative standard deviation of peak areas from 30 of the major fragments formed from a PA/PAH copolymer and polysaccharide was 20-25% (n = 10) when an experimental set up similar to that required for pyrolysis of pollen grains was used (Kaal et al., 2008). Reproducibility over long analytical periods also appears to present difficulties due to machine drift, particularly between servicing periods. Therefore, finding methods to improve the analytical precision in this method remains a key objective in the development of a pollen-based UV-B proxy.

Here, we present results from a series of tests developed to ensure a more robust and accurate methodology for analysing UV-B absorbing compounds in modern Pinus spp. pollen grains sampled from the Arboretum and Botanical Garden of Milde in Bergen, Norway. First, we demonstrate that measuring the ratio of pCA against an internal standard, Nonadecanoic acid, rather than raw concentrations, results in major improvements in the precision of our py-GC/MS when using a set of calibration

solutions. Second, we document the sporopollenin-based py-GC/MS derivatives from Pinus sylvestris L. pollen to ensure that Nonadecanoic acid is not detected in the pollen exine. Finally, we develop a modified protocol enabling us to introduce this standard to pollen samples, and apply this new protocol to test whether changes in pCA abundance can be detected in samples containing different numbers of pollen grains. The results from this study open the door for future comprehensive analytical investigations into the drivers of change of pollen-chemistry signatures in pollen in the development of a UV-B proxy.

2. Methods

2.1 Instrumental set-up and py-GC/MS conditions

For all analyses we use an HP-Agilent 6890 GC with an HP-Agilent 5973 Mass Selective Detector (MSD). The GC system was equipped with an Optic 3 PTV-injector (ATAS GL, Veldover, The Netherlands) and a PAL Combi robotic auto sampler (ATAS GL). The PTV injector was equipped with an electronic gas control unit used to supply the Helium carrier gas and the split flow. The Optic 3 PTV- injector is a liner-based injection system, requiring pollen grains to be transferred into LINEX DMI 30µl microvial (ATAS GL), before these microvials are loaded into the tapered glass liners within the pyrolysis unit. This is different to the filament injector system used in previous studies (Blokker et al., 2005; Watson et al., 2007). A filament injector would enable more efficient heat transfer from heater to sample, but requires a more complex set of attachments to transport the sample to the column and may result in memory effects between runs (Blokker et al., 2005). We soaked the glass liners in a 97:3 DCM: MeOH solution to minimise contamination between sample runs.

The GC was fitted with an HP-Ultra 25 m x 0.2 mm (internal diameter) column with a 0.33 µm film. Unless stated otherwise, column flow of the carrier gas was set to 0.9 mL/ minute and a split flow to 250 mL/minute during sample injection and 20 mL/minute thereafter. The pyrolysis heating programme was set to rise from 40°C to 600°C (maximum) at the maximum ramp rate (approximately 60°C/second). The GC oven was programmed from 40°C (6 minute hold time) to 130°C at 15°C/ minute followed by 250°C at 8°C/min, up to 320°C at 15°C/min and 1.5 min isothermal at 320°C (Willis et al., 2011). Data acquisition in scan mode was run with a start time of 3 minutes,

monitoring a mass range between m/z 50-550 at 2.94 scans /second. For selected ion mode (SIM) we measured the m/z 74 and 161 ions with a dwell time of 75 ms. We then conducted the following tests to develop further the methods underlying a pollen-based UV-B proxy for Pinus sylvestris pollen.

2.2 Analytical precision

We investigated whether introducing an internal standard prior to the THM reaction could improve analytical precision by taking into account variable reaction efficiency and gas transfer into the column. Nonadecanoic acid (NAA) is a straight chain aromatic compound methyl-benzoic acid with a similar structure to major aliphatic components of the sporopollenin. Given that we would expect chemical homologues to react in a similar way to the UV-B absorbing compounds during the THM process, we tested whether standardisation of the pCA peaks with NAA would result in improved precision in the analysis.

We prepared five calibration solutions containing ratios of approximately 1:1, 1:1.25, 1:1.5, 1:175 and 1:2 concentrations of NAA (~0.01g) and pCA (~0.01 g, 0.0125 g, 0.015 g, 0.0175 g, 0.02 g) respectively, dissolved in 0.4 ml of MeOH and 0.2 ml of 25% TMAH (in MEOH) and made up to 1 ml with MeOH. The solutions were stored at 4°C in between sample analysis. 1µl of solution was applied to the inside of the microvial using an 1µl SGE syringe with a 50mm needle and Pt#1 tip (509221). These microvials were then inserted into the LINEX liners before being subjected to py-GC/MS. We ran all samples in full-scan mode and tested whether different combinations of ratios between representative ions (m/z 161 and 191 ions: pCA; m/z 74, 87, and 312 ions: NAA) resulted in decreases in relative standard deviations (RSD) compared to raw values of the ions representative of pCA.

2.3 THM- py-GC/MS of Pinus spp. pollen

A drawn-out Pasteur pipette was used to extract pollen grains for analysis. Pollen grains had been submerged in distilled water and were extracted under a Zeiss AXIO vert.A1 inverted microscope and then transferred to 30 µl microvials, which were then centrifuged and the left overnight to dry at 50ºC. After drying, 2 µl of a solution

containing 200 µl 25% TMAH and 1000 µl MeOH was added to the sample using a Hamilton Digital syringe to the top of the microvial, before being centrifuged to ensure complete sample coverage. The wetted pollen grains were left for 20 minutes, placed in an oven 70°C for 2 hours, and then left overnight at room temperature (Willis et al., 2011). To investigate the complete set of sporopollenin-based THM derivatives, we ran 3 replicates of samples containing 200 grains of Pinus sylvestris pollen in full-scan mode and a further sample was run after adding 50 µl of an internal NAA standard solution (0.001 g NAA dissolved in 1 ml MeOH) to the TMAH solution. This test would enable us to investigate whether NAA is naturally present in the derivatives from a pollen sample. Sporopollenin derivatives were determined by comparing the associated mass spectra of major peaks using the NIST MS database (https://www.nist.gov/srd/nist-standard-reference-database-1a-v14).

2.4 Quantification of pCA in Pinus sylvestris pollen

To investigate whether samples with an increasing number of pollen grains resulted in a linear increase in the amount of pCA detected when compared against a known concentration of NAA, we prepared samples containing between 50 and 400 grains of Pinus sylvestris from the Arboretum and Botanical Garden, Milde, at the University of Bergen. We used the same pollen preparation method described above, but added 2 µl of an NAA:MeOH solution as an internal standard to the 30% TMAH before adding it to the microvials using a Hamilton 1701RN 10 µl syringe. This would ensure consistent application of NAA to each sample, against which the pCA peak could be compared. Following the results derived from the precision tests using the calibration solutions (see above), samples were run in single ion mode with detection of m/z 161 (pCA) and m/z 74 (NAA) ions.

Peak heights were detected using the MALDIquant package (Gibb and Strimmer, 2012) in R (version 3.2.1) (R Development Core Team, 2016). Before quantifying peak heights, a baseline correction procedure was used following a Statistics-Sensitive Non-Linear Iterative Peak-Clipping algorithm (Ryan et al., 1988), and the background-noise level was estimated by finding the median absolute deviation. Signal-to-noise ratios at different numbers of pollen grains were calculated by dividing the m/z 161 peak height

with 2 times the median absolute deviation of the estimated background noise level on square-root transformed data. Linear and sigmoidal models were fitted to the m/z 161: 74 ion ratios and the m/z 161 ion signal-to-noise ratio against the number of grains respectively using non-linear least squares in the nlme package (Pinheiro et al., 2013). In our tests, the initial sample at 200 grains was found to have anomalously low values of pCA so we reran this sample and report the mean value of the two samples here.

3. Results

3.1 Analytical precision

Analytical precision (as measured by the relative standard deviation, RSD) of the raw peaks of the m/z 161 ion ranged between 4.5-12.9% (mean RSD = 8.3%), and the range in RSD of the m/z 192 ion was 4.8- 13.2% (mean = 8.9%). Both these ions are representative of the pCA from the analytical standard. Standardisation of the pCA ions (m/z 161, 192) by those represented by NAA (m/z 74, 87, 312) resulted in reductions in the RSD by approximately 50% (Figure 1a, b). The best analytical precision (i.e. lowest RSD) was achieved when the m/z 161 ion (pCA) was standardized by the m/z 74 ion (NAA) (RSD between 1.1-4.0%) (Figure 1b). There was a strong linear relationship between the known ratios in the standard solutions and the ratio between the 161 and 74 ions detected in the GC (Adjusted r2 = 0.998, $p < 0.001$) (Figure 1c), although the ratio was not 1:1 because of the differing absolute amounts of the ions in the pCA vs NAA peaks.

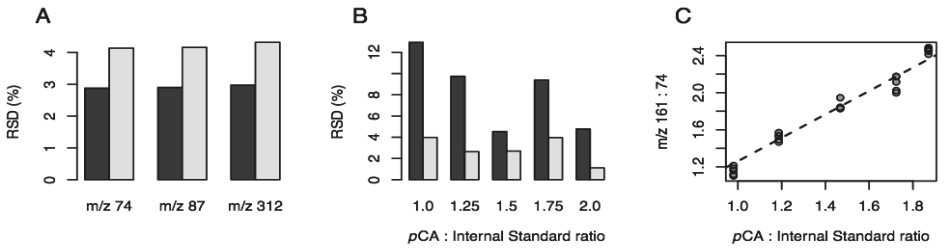

Figure 1: Results from the tests to improve analytical precision in our system set-up. **A)** Mean RSD of the m/z 161 (dark grey bars) and the m/z 192 ions (light grey bars) from the standards, divided by different ion combinations from the NAA peak (m/z 74, 87, 312). **B)** Comparisons of the RSD from the raw m/z 161 peak and the peak when standardised by the m/z 74 peak for the five different standard concentrations. **C)** Comparisons of the estimated pCA: NAA ratio compared to the known ratio in the five standard solutions using the m/z 161: 74 ion.

3.2 Pinus spp. in full scan mode

The chromatogram from the mean spectra revealed that the retention time for the main pCA peak was 17.7 minutes, with a small secondary peak at 16.7 minutes (Figure 2, Table 1). In the full scan of the Pinus sylvestris Pinus sylvestris pollen, this small secondary peak was also overlaid with an additional compound (Benzoic acid, 3,4-dimethoxy-), but extraction of the m/z 161 or m/z 192 ion would enable separation of these two compounds, so as to minimise the influence of signal interference. Ferulic acid, a second UV-B absorbing compound identified by Blokker et al. (2005) , was not detected within the 200-grain pollen samples. Other key constituents of the sporollenin included a series of aromatic compounds and long-chain fatty acids (e.g. Hexadecanoic acid, Heptadecanoic acid and Octadecanoic acid). A number of compounds, including a large peak with a retention time of 9.2 minutes (peak 4) were not possible to identify using the NIST MS database. The retention time of the internal standard (Nonadecanoic acid) in the sample containing the internal standard was 24.3 minutes (peak 30). Although this compound is a chemical homologue to other constituents of the sporopollenin it was not observed in the Pinus sylvestris pollen samples analysed without the addition of this internal standard.

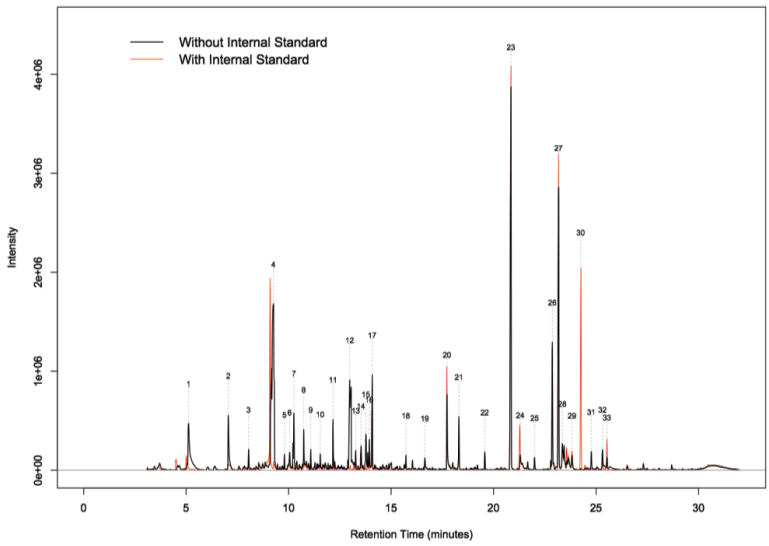

Figure 2 Full-scan chromatogram of 200 grains of Pinus sylvestris pollen. The black line is the mean chromatogram from three scans. The red line is is a chromatogram of a 200-grain sample of Pinus sylvestris with the internal standard added. Numbers for the compounds observed are provided in Table 1.

Table 1 THM-py-GC/MS derivatives of Pinus sylvestris pollen

Code	Retention Time	Compound
1	5.1	Glycine, N.N-dimethyl ester
2	7.1	Unknown Compound
3	8.0	Hexanoic acid, methyl ester
4	9.3	Unknown Compound
5	9.8	Heptanoic acid, methyl ester
6	10.0	Unknown Compound
7	10.3	Unknown Compound
8	10.7	Benzoic acid, methyl ester
9	11.1	Octanoic acid, methyl ester
10	11.5	Benzene, 1,4-dimethoxy
11	12.5	Nonanoic acid, methyl ester
12	13.0	Unknown Compound (83 ion)
13	13.3	Decanoic acid, methyl ester
14	13.6	Unknown Compound (98 ion)
15	13.8	Unknown Compound
16	13.9	Benzoic acid, 4-methoxy-, methyl ester
17	14.1	Unknown Compound (128 ion)
18	15.7	Dodecanoic acid, methyl ester
19	16.7	*para*-Coumaric acid + Benzoic acid, 3, 4-dimethoxy-, methyl ester
20	17.7	*para*-Coumaric acid
21	18.3	Tridecanoic acid, 12-methyl-, methyl ester
22	19.6	Pentadecanoic acid, methyl ester
23	20.9	Hexadecanoic acid, methyl ester
24	21.5	Hexadecanoic acid, 14-methyl-, methyl ester
25	22.0	Heptadecanoic acid, methyl ester
26	22.9	9-Octadecenoic acid, methyl ester, (E)-
27	23.1	Octadecanoic acid, methyl ester
28	23.3	7,10-Octadecadienoic acid, methyl ester
29	23.8	7,10-Octadecadienoic acid, methyl ester
30	24.3	Nonadecanoic acid, methyl ester (Internal Standard)
31	24.7	Unknown Compound
32	25.4	Eicosanoic acid, methyl ester
33	25.6	1-Phenanthrenecarboxylic acid, 1,2,3,4,4

3.3 Quantification of pCA in Pinus sylvestris

The relationship between the standardised pCA: NAA ratio and the number of grains added to the sample was strongly linear (Adjusted r2 = 0.958, $p < 0.001$) (Figure 3a). The slope of the regression was highly significant and indicates the capability of the ratio method to detect changes in pCA. The signal-to-noise ratio begins to plateau after 250 grains (Figure 3b), although signal-to-noise ratios were still generally high on the square-root transformed data at 150 grains, and so would still likely be sufficient for quantitative analysis in sediment samples with low numbers of pollen grains.

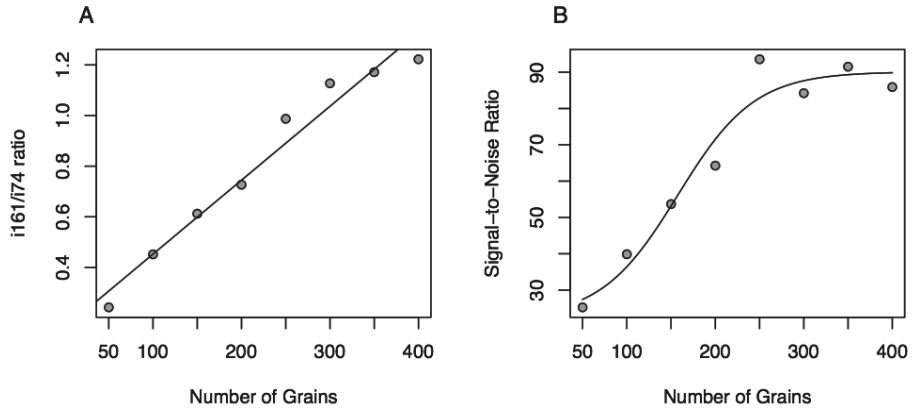

Figure 3 A) Estimated p-CA: NAA ratio (m/z 161 intensity) measured against the number of grains loaded into the sample. **B)** Signal-to-noise ratio of m/z 161 in relation to the number of grains.

4. Discussion

4.1 Improvements to reproducibility

The first tests in this study aimed to investigate whether sample reproducibility could be improved through measuring the relative ratios of pCA and NAA, rather than raw pCA values, using a set of pre-mixed calibration solutions. We found reductions in RSD of approximately 50% when the ratio between m/z 161 and m/z 74 was used (Figure 1). These results are better than those previously reported from a similar system (Kaal et al., 2008) and indicate the strong potential of the method for accurate determination of pCA abundances within pollen grains.

Sample reproducibility is a known problem in TMH with py-GC-MS. Kaal et al. (2008) suggested that low reproducibility in their analysis was potentially the result of poor mixing between sample and analyte, and found that RSD was reduced to around 6-7% when a liner that would encourage more mixing of analyte and THM solvent within the py-GC/MS set-up was used. Because our standards were premixed with TMAH, we did not expect mixing of analyte and reagent to be the key issue in reducing reproducibility in this experimental setup. This may explain the generally lower RSD compared to Kaal et al. (2008) even when unstandardised pCA peaks were assessed in this study.

Since NAA is a carboxylic acid, we expect it to have a similar reaction efficiency as pCA (and other similar compounds) released from the sporopollenin. As a result, we

also expect it to behave in a similar way in the TMAH reaction. These comparable parallel efficiencies for the different compounds are likely to be a major reason why standardisation by NAA resulted in reductions in the RSD. Further reductions may be also have been achieved through the correction of any variations in the sample transfer from the pyrolysis chamber into the GC column. Taken together, the results show the strong potential for improved analytical precision for the py-GC/MS analysis of sporopollenin components when comparisons against the internal NAA standard are used.

4.2 Sporopollenin components of Pinus sylvestris

The mean total ion content of the Pinus sylvestris samples indicates that its sporopollenin derivatives contained a combination of aromatic compounds, long-chain fatty acids and a number of compounds that could not be identified using the NIST MS database (Figure 2). Crucially we did not find evidence of NAA in any of the full scan pollen samples run for this study. This is important, because it means that if added as an external compound during the sample preparation stage it will not interact with other derivatives in the py-GC/MS reaction.

The results of the full scans of Pinus sylvestris pollen (Figure 2) were similar when compared to the full scan of acetolysised Alnus spp. pollen (Blokker et al., 2005). As indicated for Alnus spp., pCA represents an important part of the THM residue, although we found a consistent separation of this compound between two different retention times, at 16.7 and 17.7 minutes, in approximately the ratio of1:10 (Figure 2). This is probably the result of the stereochemistry of para-Coumaric acid, which can exist in two isomeric forms due to its double bond. If there is rotation during the THM reaction, the hydrogen and acid group change places and a mixture of the original trans conformation and the alternative cis conformation will result. These compounds have different properties, potentially resulting in the separation of the different compound derivatives in the final chromatogram.

In contrast to the results of Alnus spp. pollen (Blokker et al., 2005), we found no evidence of Ferulic acid in Pinus sylvestris when using pollen sums that could realistically have been extracted from a sediment core (although Ferulic acid was

observed when we analysed a raw pollen sample with a large number of grains (estimated < 10,000)). This has implications for the use of the method in UV-B proxy. As an alternative to using absolute values detected in the py-GC/MS analysis, Blokker et al. (2005) proposed using the ratio between pCA and Ferulic acid to detect differences in pollen chemistry across UV-B gradients, since the two compounds appeared to respond in different ways to UV-B exposure. Although they did not find that precision improved compared to using absolute values, a ratio approach would potentially remove the necessity to count a precise number of pollen grains within each sample. Our results indicate that such an approach would not be possible when using Pinus sylvestris pollen. As a result, the next best methodological procedure would be to measure ratios between the pCA and the internal NAA standard within each pollen sample.

4.3 Quantification of pCA

Our final analysis aimed to test whether a ratio approach could be extended to quantify pCA in Pinus sylvestris pollen grains. Results from this analysis showed a linear relationship between the number of grains and the ratio of pCA: NAA in samples with increasing numbers of pollen grains, indicating the potential for this method to be used to in a pollen-based UV-B proxy.

In order to obtain these results, we were required to make series of modifications to the Blokker et al. (2005) procedure. First, rather than transferring pollen grains to the side of the microvial, leaving it to dry and then counting, we preferred a method in which we applied pollen samples to vial before centrifuging. Second, we applied a fixed amount of TMAH solution containing a known quantity of NAA to be used for standardisation purposes. Although this method means there are some small uncertainties related to the total number of grains transferred to the microvial, we preferred our adapted centrifuge method because it enabled more precise application of the TMAH solution to the sample before pyrolysis compared to that proposed by Blokker et al. (2005). Furthermore, during preliminary tests, we checked whether the number of pollen grains that were successfully transferred to the bottom of the microvial by comparing the expected (i.e. 50) vs. observed number of grains in the pollen pellet in 10 samples after centrifugation. The maximum was 52 grains and the minimum was 45 with a mean of 48 (sd 2.68, n=

10). We expect that this uncertainty is likely to be small relative the variability observed in natural populations. In addition, this uncertainty could be incorporated in any further statistical analyses by using hierarchical modelling approaches (Jokerud et al., submitted). To summarise these methodological changes we provide an adapted protocol in the supplementary material of this paper.

4.4 Implications and Outlook

There is an emerging interest in using pollen chemistry to reconstruct changes in UV-B, and our study has major implications for the robustness of any method attempting to apply such approaches to the fossil record. Potential applications of the technique range from using pollen chemistry to investigate changes in solar variability and cloud cover on millennial timescales (Lomax et al., 2008; Magri, 2011; Willis et al., 2011), and to investigate the evolutionary and ecological impacts of UV-B changes on plants across major geological boundaries (Beerling et al., 2007; Looy et al., 2001; Visscher et al., 2004; Willis et al., 2009). The adapted methodology presented in this paper lays the foundations for more robust data analysis when using pollen chemistry for these applications. Since these analyses would be required to run a large number of samples (i.e. > 100) over a long-time period (i.e. a number of months), we also expect that the internal standard will be a useful tool to correct for machine drift (e.g. between servicing periods), and hence provide additional capabilities for reproducibility across large datasets. We suggest that regular cleaning of the pyrolysis unit, in addition to cuts to the column to remove build up of pyrolysis residues may be critical for this standardisation. In addition, our results so far may indicate that the method may be sensitive to evaporation of the TMAH/ NAA solution, so regular refreshing of standards may be necessary. The optimal frequency for these methods to achieve this long-term standardisation are currently being explored.

The fact that major differences in the sporopollenin-based derivatives of Pinus sylvestris were so different to those observed in Alnus highlights important future research directions. Firstly, the concentrations of UV-B absorbing components appear to differ between genera, since Ferulic acid is not found in large abundances in Pinus sylvestris pollen as compared to Alnus spp. In addition, although the composition of

sporopollenin-based derivatives were generally similar between different Pinus species, Jokerud et al. (submitted) identified clear differences in the absolute values of the different compounds, including pCA, which were only partly explained by pollen size. Combined, these results highlight the importance of developing species-specific pollen-chemistry proxies for UV-B since the THM derivatives, and the relationships between these derivatives, may differ.

Second, an additional future step in the development of a pollen-based proxy will be to investigate whether it is possible to devise quantitative reconstructions of past UV-B. Critical questions that remain unanswered related to this include understanding the period of the year over which the UV-B absorbing compounds respond to UV-B exposure (e.g. Jokerud et al., submitted), and how best a dose-response relationship can be quantified. For example, whether a dose-response relationship is best determined through latitudinal or elevational gradient studies (Jokerud et al., submitted), or through field- or laboratory- based experimental studies (Jokerud et al., submitted) remains an open question. Since the full scan analysis of Pinus sylvestris revealed a number of other additional aliphatic and aromatic components within the sporopollenin (Figure 2), it would also be interesting to investigate whether these additional components can be used to improve these precision estimates through multivariate approaches.

Finally, a potential future use of the full spectrum of compounds in the THM reaction of pollen grains is in chemo-taxonomy, by investigating taxonomic differences between genera within pollen grains using modern samples. So far this field has mainly used FTIR or Raman spectroscopic methods (Ivleva et al., 2004; Zimmermann and Kohler, 2014; Zimmermann, 2010), and results from these studies indicate that variations between the lipid and sporopollenin ratio within pollen can be used to distinguish between different plant genera. However, the preservation potential of such lipids, once submerged under water and buried in sediments, is expected to be poor and so whether such methods could be applied to sub-fossil samples from lakes and bogs remains unknown. The fact that detectable differences within the sporopollenin is observed is promising, since it shows that the preservable, sub-fossilised material within genera may also be used to investigate taxonomic differences. Future studies should seek to combine

methodologies to further explore the potential of sporopollenin-only species-specific differences for chemo-taxonomic purposes in a palaeoecological context.

5. Conclusions

In this study we present an adapted methodology for analysing UV-B absorbing compounds in Pinus spp. pollen grains. Although achieving precision using standard pyrolysis systems is challenging, our method ensures more precise quantitative determination of UV-B absorbing compounds in Pinus sylvestris pollen. We used this method to detect linear increases in the total amount of pCA in samples containing different numbers of pollen grains. Analysis of the chromatograms revealed differences in the chemical spectra of P. sylvestris pollen grains, indicating that analyses should be carefully designed for specific plant genera. We anticipate that in the future the method proposed in this paper will aid quantification of uncertainties for pollen-based palaeo-UV-B reconstructions, and for the emerging field of research into using pollen-chemistry techniques in a suite of other palynological and palaeobotanical investigations.

6. Funding

This work was was provided by the Research Council of Norway (FRIMEDBIO 214359, 249844).

7. References

Beerling, D.J., Harfoot, M., Lomax, B., Pyle, J.A., 2007. The stability of the stratospheric ozone layer during the end-Permian eruption of the Siberian Traps. Philosophical Transactions of the Royal Society A: Mathematical, Physical and Engineering Sciences 365, 1843–1866. doi:10.1016/j.tig.2005.01.002

Blokker, P., Boelen, P., Broekman, R., Rozema, J., 2006. The occurrence of p-coumaric acid and ferulic acid in fossil plant materials and their use as UV-proxy. Plant Ecology. doi:10.1007/s11258-005-9026-y

Blokker, P., Yeloff, D., Boelen, P., Broekman, R.A., Rozema, J., 2005. Development of a Proxy for Past Surface UV-B Irradiation: A Thermally Assisted Hydrolysis and

Methylation py-GC/MS Method for the Analysis of Pollen and Spores. Analytical Chemistry 77, 6026–6031. doi:10.1021/ac050696k

Challinor, J.M., 2001. Review: the development and applications of thermally assisted hydrolysis and methylation reactions. Journal of Analytical and Applied Pyrolysis 61, 3–34.

De Leeuw, J.W., Versteegh, G.J.M., van Bergen, P.F., 2006. Biomacromolecules of Algae and Plants and Their Fossil Analogues. Plant Ecology 182, 209–233.

Foster, C.B., Afonin, S.A., 2005. Abnormal pollen grains: an outcome of deteriorating atmospheric conditions around the Permian–Triassic boundary. Journal of the Geological Society, London 162, 653–659.

Fraser, W.T., Scott, A.C., Forbes, A.E.S., Glasspool, I.J., Plotnick, R.E., Kenig, F., Lomax, B.H., 2012. Evolutionary stasis of sporopollenin biochemistry revealed by unaltered Pennsylvanian spores. New Phytologist 196, 397–401. doi:10.1111/j.1469-8137.2012.04301.x

Gao, W., Schmoldt, D., Slusser, J.R., 2010. UV Radiation Global Climate Change: Measurements, Modeling and Effects on Ecosystems 550.

Gibb, S., Strimmer, K., 2012. MALDIquant: a versatile R package for the analysis of mass spectrometry data. Bioinformatics 2270–2271.

Ivleva, N.P., Niessner, R., Panne, U., 2004. Characterization and discrimination of pollen by Raman microscopy. Analytical and Bioanalytical Chemistry 381, 261–267. doi:10.1007/s00216-004-2942-1

Jardine, P.E., Fraser, W.T., Lomax, B.H., Gosling, W.D., 2015. The impact of oxidation on spore and pollen chemistry. Journal of Micropalaeontology 34, 139–149. doi:10.1144/jmpaleo2014-022

Jokerud, M., Seddon, A.W.R., Barth, T., Birks, H.J.B., Vandvik, V., Willis, K.J., (submitted). Short-term, plastic response to UV-B radiation across Europe, obtained by using UV-B absorbing compounds in pollen of Pinus sylvestris.

Jokerud, M., Seddon, A.W.R., Willis, K.J., Vandvik, V., (submitted) Plastic responses and species-level variation of UV-B absorbing compounds in Pinus spp. to short-term variation in UV-B radiation.

Kaal, E., de Koning, S., Brudin, S., Janssen, H.-G., 2008. Fully automated system for the gas chromatographic characterization of polar biopolymers based on thermally

assisted hydrolysis and methylation. Journal of Chromatography A 1201, 169–175. doi:10.1016/j.chroma.2008.05.047

Lomax, B.H., Fraser, W.T., 2015. Palaeoproxies: botanical monitors and recorders of atmospheric change. Palaeontology 58, 759–768. doi:10.1111/pala.12180

Lomax, B.H., Fraser, W.T., Harrington, G., Blackmore, S., Sephton, M.A., Harris, N.B.W., 2012. A novel palaeoaltimetry proxy based on spore and pollen wall chemistry. Earth and Planetary Science Letters 353-354, 22–28. doi:10.1016/j.epsl.2012.07.039

Lomax, B.H., Fraser, W.T., Sephton, M.A., Callaghan, T.V., Self, S., Harfoot, M., Pyle, J.A., Wellman, C.H., Beerling, D.J., 2008. Plant spore walls as a record of long-term changes in ultraviolet-B radiation. Nature Geoscience 1, 592–596. doi:10.1038/ngeo278

Looy, C.V., Twitchett, R.J., Dilcher, D.L., Van Konijnenbyrg-van Cittert, J.H.A., Visscher, H., 2001. Life in the end-Permian dead zone. Proceedings of the Academy of Natural Sciences of Philadelphia 98, 7879–7883. doi:10.1073 pnas.131218098

Magri, D., 2011. Past UV-B flux from fossil pollen: prospects for climate, environment and evolution. New Phytologist 192, 310–312.

Pinheiro, J., Bates, D., Debroy, S., Sarkar, D., and the R Development Core Team., 2013. nlme: Linear and Nonlinear Mixed Effects Models. [WWW Document]. URL http://CRAN.R-project.org/package=nlme/

Rozema, J., Noordijk, A.J., Broekman, R.A., van Beem, A., Meijkamp, B.M., de Bakker, N.V.J., van de Staaij, J.W.M., Stroetenga, M., Bohncke, S.J.P., Konert, M., Kars, S., Peat, H., Smith, R.I.L., Convey, P., 2001. (Poly)phenolic compounds in pollen and spores of Antarctic plants as indicators of solar UV-B – A new proxy for the reconstruction of past solar UV-B? Plant Ecology 154, 9–26. doi:10.1023/A:1012913608353

Ryan, C.G., Clayton, E., Griffin, W.L., Sie, S.H., Cousens, D.R., 1988. Snip, a statistics-sensitive background treatment for the quantitative analysis of pixe spectra in geoscience applications. Nuclear Instruments & Methods in Physics Research Section B-Beam Interactions with Materials and Atoms 3, 396–402.

R Core Team, 2016. R: A language and environment for statistical computing. [WWW Document]. URL http://www.R-project.org/

Visscher, H., Looy, C.V., Collinson, M.E., Brinkhuis, H., Van Konijnenbyrg-van Cittert, J.H.A., Kürschner, W.M., Sephton, M.A., 2004. Environmental mutagenesis

during the end-Permian ecological crisis. Proceedings of the Academy of Natural Sciences of Philadelphia 101, 12952–12956. doi:10.1073 pnas.0404472101

Watson, J.S., Sephton, M.A., Sephton, S.V., Self, S., Fraser, W.T., Lomax, B.H., Gilmour, I., Wellman, C.H., Beerling, D.J., 2007. Rapid determination of spore chemistry using thermochemolysis gas chromatography-mass spectrometry and micro-Fourier transform infrared spectroscopy. Photochemical & Photobiological Sciences 6, 689. doi:10.1039/b617794h

Willis, K.J., Bennett, K.D., Birks, H.J.B., 2009. Variability in thermal and UV-B energy fluxes through time and their influence on plant diversity and speciation. Journal of Biogeography 36, 1630–1644. doi:10.1111/j.1365-2699.2009.02102.x

Willis, K.J., Feurdean, A., Birks, H.J.B., Bjune, A.E., Breman, E., Broekman, R., Grytnes, J.-A., New, M., Singarayer, J.S., Rozema, J., 2011. Quantification of UV-B flux through time using UV-B-absorbing compounds contained in fossil Pinus sporopollenin. New Phytologist 192, 553–560. doi:10.1111/j.1469-8137.2011.03815.x

Zimmermann, B., 2010. Characterization of Pollen by Vibrational Spectroscopy. Applied Spectroscopy 64, 1–10.

Zimmermann, B., Kohler, A., 2014. Infrared Spectroscopy of Pollen Identifies Plant Species and Genus as Well as Environmental Conditions. PloS one 9, e95417. doi:10.1371/journal.pone.0095417.s001

Appendix

IV

Table A1. Beug (1961)'s average Pinus spp. pollen size and calculated biovolume.

Species	Average size	Biovolume
P. cembra	84.4	5 592
P. mugo	69.2	3 759
P. nigra	73.3	4 218
P. peuce	82.0	5 278
P. pinaster	96.0	7 235
P. sylvestris	73.5	4 241
P. uncinata	69.2	3 759

Figure A1. Microscope photos of Pinus species.

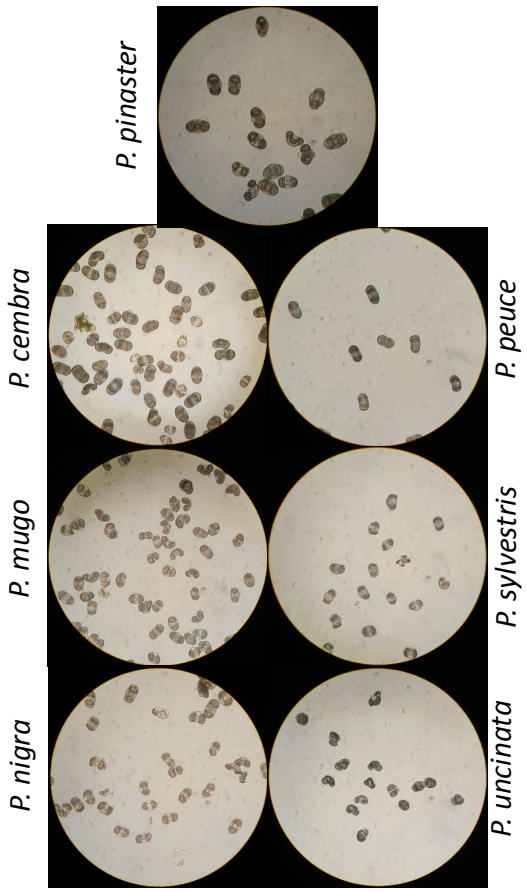

Figure A1. Photo of *Pinus* spp. pollen under under a Leica DMIL 090-135.001 inverted microscope with objective x20

A2. Bayesian hierarchical models

We used a hierarchical model in **Paper II** and **III** to test for differences in i) *p*CA quantity between shaded and sun-exposed pollen of *Pinus sylvestris* using a multilevel model with trees as random effects and treatment as fixed effects, ii) *p*CA quantity between pollen produced in 2013 and 2014 and iii) variability of *p*CA in different *Pinus* species under equal UVB-influx conditions using a main-effects ANOVA model with trees as random effects. (Gelman and Hill, 2007). Parameters of the model were estimated using Bayesian inference. The model (likelihood) was designed to characterise uncertainty at different parts of the analytical process and was based on three main components.

Our first component (Equation 1.1) characterises the uncertainty in the analytical measurements of the py-GC/MS process. Preliminary tests have indicated imperfect detection of *p*CA ratios due to unavoidable varying reaction efficiencies and potential minor contamination (Seddon *et al.* submitted). Therefore, we assume the measured *p*CA ratio of a sample, *y*, to be drawn from a Gamma distribution whose parameters are defined by $shape_{\mathrm{GC}}$ (α_{GC}), and the actual *p*CA ratio of the pollen sample, y_{ratio}. (Equation 1.1). The parameters for $shape_{\mathrm{GC}}$ are based on measurements from the variance of standards run at two-sample intervals over the course of the analysis and are set as informative priors (see Supporting Information). The value y_{ratio} is calculated as the product of ${}_{n}\mathrm{Grains}$, the number of grains in a sample and μ_{ratio}, the mean effect of a treatment on the *p*CA on one pollen grain in a sample (Equation 1.2).

Equation 1.1: $y_{\mathrm{obs}} \sim \mathrm{Gamma}\left(\alpha_{\mathrm{GC}} \frac{\alpha_{\mathrm{GC}}}{\mathrm{y}_{\mathrm{ratio}}}\right)$

Equation 1.2: $y_{\mathrm{ratio}} = {}_{n}\mathrm{Grains} * \mu_{\mathrm{ratio}}$

The second component estimates the value of ${}_{n}\mathrm{Grains}$, for which we use a Gaussian distribution rounded to the nearest whole number (Equation 2.1), where *n* is the target number of grains picked from the sample, and $\sigma\ {}_{n}\mathrm{Grains}$ is the standard deviation of *n*. This model is necessary since small errors can be made when picking and loading *n* number of grains into a microvial. The value $\sigma\ {}_{n}\mathrm{Grains}$ is set as an informative prior,

the parameters of which are estimated from a previous analysis (see Supporting Information).

Equation 2.1: $_n\text{Grains} \sim DN_0\left(n,\ \sigma\ _n\text{Grains}\right)$

where $\mathbb{P}\left(\ _n\text{Grains} \mid \text{n},\ \sigma\ _n\text{Grains}\right)$

$= \phi_0(\ _n\text{Grains}, +0.5, n, \sigma\ _n\text{Grains}) - \phi_0(max(\ _n\text{Grains}, +0.5), n, \sigma\ _n\text{Grains})$

Truncated normal distribution function:

$$\phi_0(x, \mu, \sigma) = \frac{\phi\left(\frac{x-\mu}{\sigma}\right)}{\left[1 - \phi\left(\frac{0-\mu}{\sigma}\right)\right]}$$

$$= \frac{\int_{-\infty}^{\frac{x-\mu}{\sigma}} e^{-\frac{t^2}{2}}\, dt}{\left[\sqrt{2\pi} - \int_{-\infty}^{\frac{\mu}{\sigma}} e^{-\frac{t^2}{2}}\, dt\right]}$$

The final component describes the mean effect of a treatment on the *p*CA on one pollen grain in a sample and is used to calculate μ_{ratio}. We assume this is drawn from a Gamma distribution with parameters $shape_{\text{pollen}}(\alpha_{\text{pollen}})$ and μ_{pollen} (Equation 3.1).

Equation 3.1 $\mu_{\text{ratio}} \sim \text{Gamma}\left(\alpha_{\text{pollen}}, \frac{\alpha_{\text{pollen}}}{\mu_{\text{pollen}}}\right)$

We use an uninformative prior to estimate the value of $shape_{\text{pollen}}$ of used linear mixed effects models (Gelman & Hill, 2007) in both experiments to estimate μ_{pollen}. For experiment 1 (i.e. plastic effects in *Pinus sylvestris* from Bergen), our goal was to estimate the difference β, between the two treatments (i.e. sun or shaded), where μ_{pollen} is the effect of treatment on the *p*CA ratios within the pollen, α_i is the random intercept for a given tree, i (i = 1,..,10) (Equation 3.2, Fig. A2).

Equation 3.2: $\ln\left(\mu_{\text{pollen}}\right) = \alpha_i,\ \beta * \text{treatment}$

For experiment 2 (i.e. species-level variation in Geneva), our goal was to estimate the difference δ, between years and also whether there were differences between species, where μ_{pollen} is the effect of year on the *p*CA ratios within the pollen, α_i is the random

intercept for a given tree, *i* (*i* = 1,..,8) (Equation 3.3, Fig. A2).

Equation 3.3: $\ln(\mu_{\text{pollen}}) = \alpha[\text{tree}_i] + \delta[\text{year}_i] + \delta[\text{species}_i]$

For Europe (i.e. the timing of the response of *p*CA production), our goal was to estimate the slope δ, of the different UV-B predictor variables, where μ_{pollen} is the effect of UV-B on the *p*CA ratios within the pollen, α_i is the random intercept for a given tree, *i* (*i* = 1,..,10) (Equation 3.4, Fig. A2).

Equation 3.4: $\ln(\mu_{\text{pollen}}) = \alpha_i,\ \beta * \text{uv}$

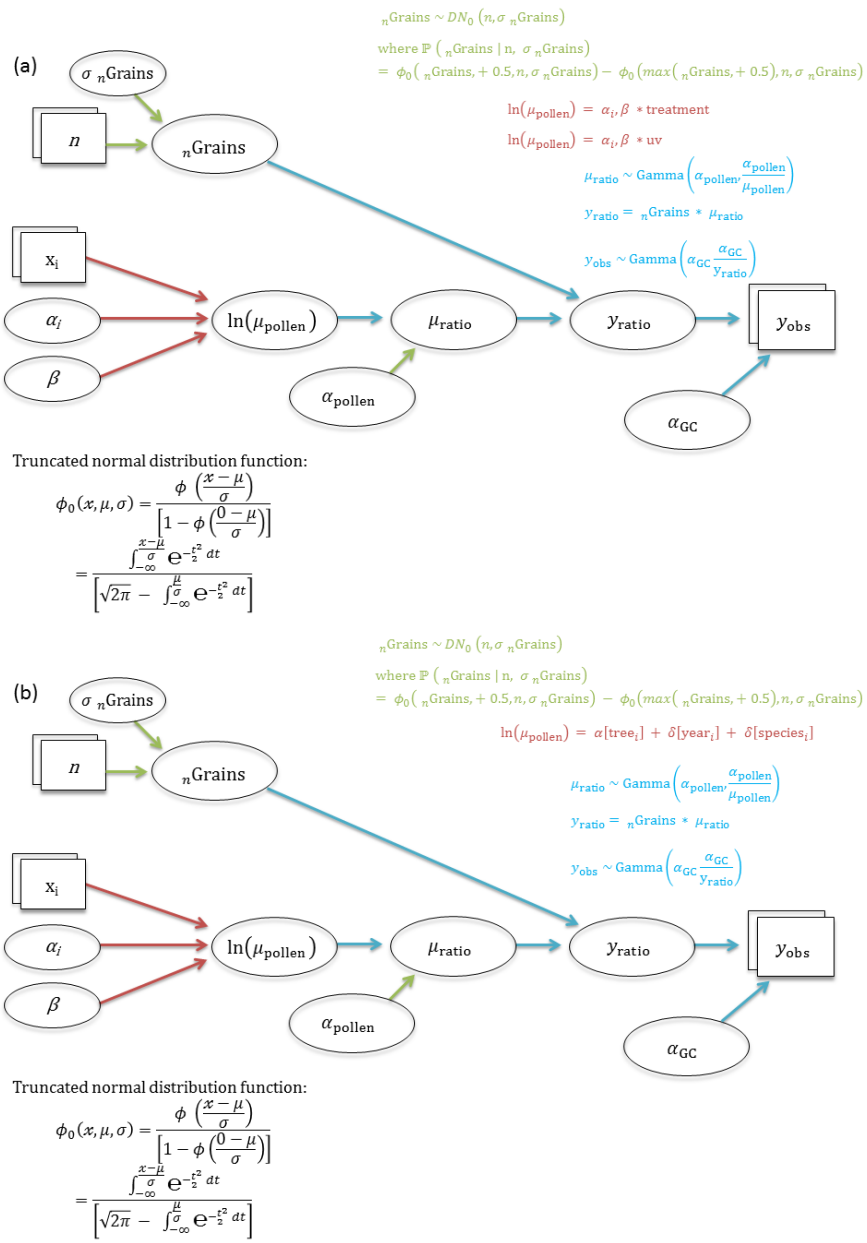

Figure A2. Mathematical description of our Bayesian hierarchical model incorporating a process model for the shading experiment (red) and analytical sub models (blue) with informative priors (green). **a)** The shading experiment and the timing of the UV-B response across Europe. **b)** The two-year comparison in

A3. Supporting Information to Paper I, S1. Adapted Protocol for sample preparation for THM py-GC/MS analysis of Pinus spp. pollen

Preparing pipette tips for pollen picking

1) Take a glass pasteur pipette (we use BRAND 230 mm, Cat. Nu. 7477 10, IS 7712) and heat the tip under a Bunsen flame. Holding the pipette at either end, roll it in your fingers until it starts to feel soft at the point under the flame.
2) At this point, draw the pipette away from the flame and pull outwards at the same time, so that the pipette narrows to a finer point.
3) Pull the two ends of the pipette apart. The pipette should split at the weakest (finest point), leaving you with a rounded, fine pipette tip that is ideal for picking pollen under a microscope. Practice this a few times to get a feel for how narrow the pipette needs to be for ideal pollen picking.
4) Attach a plastic tube to the top end of the pipette tip, and then place a 1000 ml Eppendorf (or similar) tip into this to use as a mouth piece. This pipette is now ready to pick pollen.

Pollen Picking

1) Transfer some pollen sample into a 2 ml plastic micro-tube and top up with distilled water.
2) Pollen taken from modern flowers tend to float on the top of the water, so seal the plastic tube, shake, and place in a micro centrifuge. Spin for around 1 minute, stir the pollen suspension, and re-centrifuge. Repeat this until enough pollen has been successfully submerged and is sitting on the bottom of the plastic micro-tube.
3) Place 50 µl distilled water on a welled microscope slide, extract 8 µl of this pollen suspension and add to the well, top up this well with another 50 µl of distilled water and then place on an inverted microscope.
4) Take in small enough distilled water into the pipette to prevent large amounts of pollen/ non pollen material from rushing into the pipette by capillary action when it is first placed within the pollen suspension on the slide under the microscope.

5) Pick 50 grains and transfer to another microscope well containing ~ 100 µl of water. Repeat until you have obtained the desired sum. Transferring the second well ensures that a cleaner sample, with only pollen grains, can be obtained in the next round of picking. However, if pollen sample is completely clean this step can be ignored.
6) Re-pick the grains from the second microscope well until the desired pollen sum is achieved. Transfer to the Linex micro vial from the pipette, place the micro vial into a 2 m plastic micro tube and then centrifuge so that the pollen collects at the bottom of the micro vials. Note that we have found the most accurate results when pollen is transferred to the micro vial 50 grains at a time. i.e. if 200 grains are to be transferred then do 4 x 50 grain transfers to the micro vial.
7) Place the micro vials in an oven at 50ºC and leave overnight to allow the water to evaporate.
8) If the pollen sample in the plastic tube is used another day, dry the pollen at 50º in oven to avoid microbe growth.

TMAH preparation

1) Prepare a TMAH : Nonadecanoic acid (NAA) solution (see Methods section in main paper for concentrations). We use a solution containing 200 µl 25% TMAH and 1000 µl MeOH, in addition to 50 µl of an internal NAA standard solution (0.001 g NAA dissolved in 1 ml MeOH) to the TMAH solution
2) Use a digital syringe (we use a Hamilton Digital 1701RN 10µl syringe), pre-set to deliver 2 µl of the TMAH: NAA solution.
3) To ensure the syringe is clean, wash with methanol 5 times before taking up TMAH solvent
4) Apply 2 µl of the solution to the top corner of the micro vial. Repeat for up to 5 micro vials.
5) Place the vials in a 2 ml micro-tube and centrifuge for 30 510 seconds to ensure the TMAH: NAA solution is covering the pollen grains found at the bottom of the micro vial.

6) Wash the syringe 5 times with MEOH and repeat for another set of up to 5 samples.
7) When the TMAH: NAA solution has been applied to all samples, remove from the micro-vials and leave to stand for 20 minutes to allow the MEOH to evaporate.
8) Place the aluminium stand into a 70ºC oven, loosely cover it (we use an old Eppendorf pipette tip box) and then incubate for 2 hours.
9) Remove the samples and leave to stand overnight. The micro vials are then ready for py-GC/MS.

Please see the relevant section in Paper I for pyrolysis, GC-oven and MS detector conditions.

A4. Instrumental set up and py-GC/MS conditions

For all thermally assisted methylation (THM) reaction with pyrolysis-Gas Chromatography Mass Spectrometry (py-GC/MS) analyses we used an HP-Agilent 6890 GC with an HP-Agilent 5973 Mass Selective Detector (MSD). The GC system was equipped with an Optic 3 PTV-injector (ATAS GL, Veldover, The Netherlands) and a PAL Combi robotic auto sampler (ATAS GL). The PTV injector was equipped with an electronic gas control unit used to supply the Helium carrier gas and the split flow. The Optic 3 PTV- injector is a liner-based injection system, requiring pollen grains to be transferred into LINEX DMI 30µl microvial (ATAS GL), before these microvials are loaded into the tapered glass liners within the pyrolysis unit. We soaked the glass liners in a 97:3 DCM: MEOH solution to minimize contamination between sample runs.

For all analyses we used an HP-Ultra 25 m x 0.2 mm (internal diameter) column with a 0.33 µm film, with a He carrier gas. Column flow of the carrier gas was set to 0.9 ml/ minute and a split flow to 250 ml/minute during sample injection and 20 ml/minute thereafter. The pyrolysis heating programme was set to rise from 40°C to 600°C (maximum) at the maximum ramp rate (approximately 60°C / sec). The GC oven was programmed from 40°C (6 minute hold time) to 130°C at 15°C/ minute followed by 250°C at 8°C/min, up to 320°C at 15°C/min and 1.5 min isothermal at 320°C (Willis et al., 2011). Data acquisition in scan mode was run with a start time of 3 minutes,

monitoring a mass range between 50 and 550 Dalton at 2.94 scans /second. For selected ion mode (SIM) measured the ions m/z 74 and m/z 161 with a dwell time of 75 ms. This method was initially developed by Blokker et al. (2005).

First, the LINEX liners are run for 5 min in the pyrolysis unit and heated to 600° as part of the cleaning procedure. Then the microvials were then inserted into the LINEX liners before being subjected to py-GC/MS. A calibration solution is run between very second pollen sample to detect and correct for machine precision between batch and column cut. In addition, a blank sample is run after every ten samples to flush out column residue. After approximately 100 runs we clean the inside of the pyrolysis unit and cut the front 50 cm of the GC column. This is due to build-up of residue in both the pyrolysis unit and GC column after sample heat up and transfer, which in turn affects the analytical precision.

A5. Laboratory photos.

Figure A5. Laboratory photos. Top left: Microvial with prepared pollen sample ready to be placed in the LINEX liner. Top middle left: Solution of TMAH and the internal standard (NAA). Top middle right: *Pinus mugo* pollen under the microscope. Top right: Lab selfie of picking pollen. Bottom: the pyrolysis-Gas Chromatography Mass Spectrometry (py-GC/MS) units and the robotic auto sampler.

A6. Supporting Information Paper III

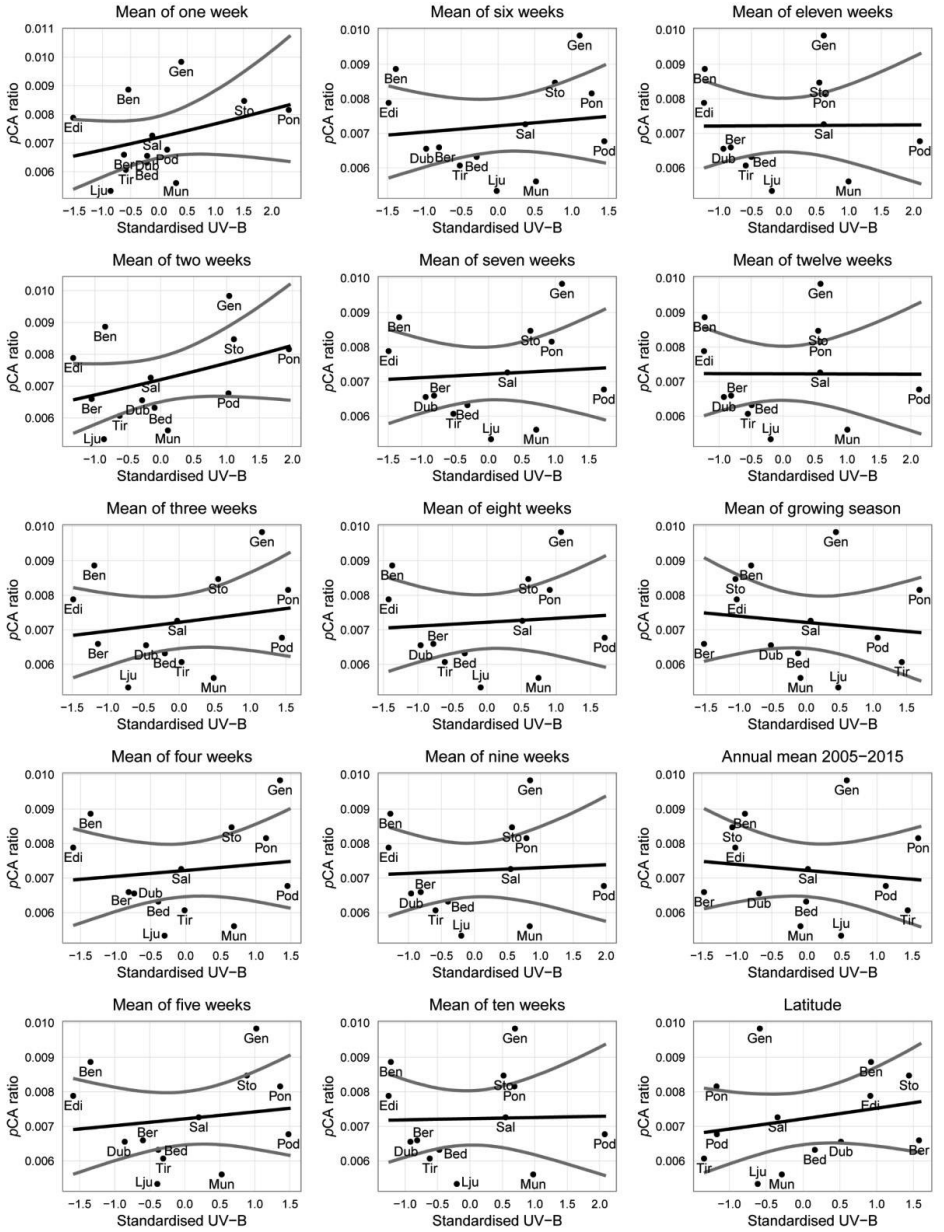

Fig. SI1. Measured p-coumaric acid (pCA) ratios in black circles. Linear regression models of the timing of the response of pCA production in Pinus sylvestris pollen across Europe using the full dataset with Benmore and Edinburgh. The regression line is calculated from the posterior estimates of the model (black) on predicted pCA production in Pinus sylvestris with a 95% credible interval (grey lines).

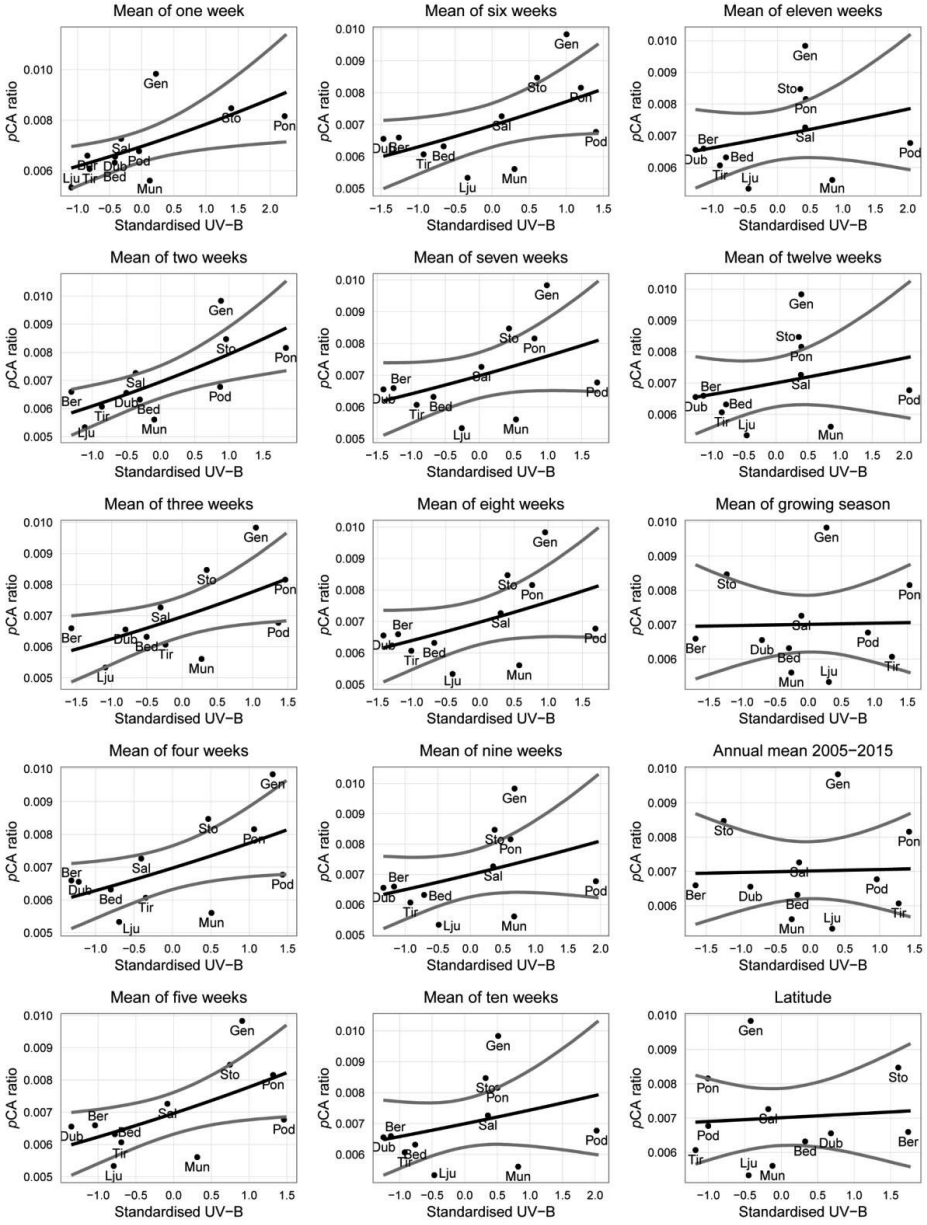

Fig. SI2. Measured p-coumaric acid (pCA) ratios in black circles. Linear regression models of the timing of the response of pCA production in Pinus sylvestris pollen across Europe using the reduced dataset without Benmore and Edinburgh. The regression line is calculated from the posterior estimates of the model (black) on predicted pCA production in Pinus sylvestris with a 95% credible interval (grey lines).